Nanocarriers for drug delivery to the inner ear: Physicochemical key parameters, biodistribution, safety and efficacy

Céline Jaudoin, Florence Agnely, Yann Nguyen, Evelyne Ferrary, Amélie Bochot

Nanocarriers for drug delivery to the inner ear: physicochemical key parameters, biodistribution, safety and efficacy

Céline JAUDOIN[a], *Florence AGNELY*[a], *Yann NGUYEN*[b,c], *Evelyne FERRARY*[b], *Amélie BOCHOT**[a]

[a] Université Paris-Saclay, CNRS, Institut Galien Paris-Saclay, 5 rue J-B Clément, 92296 Châtenay-Malabry, France. celine.jaudoin@universite-paris-saclay.fr, florence.agnely@universite-paris-saclay.fr, amelie.bochot@universite-paris-saclay.fr

[b] Inserm/Institut Pasteur, Institut de l'audition, Technologie et thérapie génique pour la surdité, 63 rue de Charenton, 75012 Paris, France. evelyne.ferrary@inserm.fr

[c] Sorbonne Université, AP-HP, GHU Pitié-Salpêtrière, DMU ChIR, Service ORL, GRC Robotique et Innovation Chirurgicale, Paris, France. yann.nguyen@inserm.fr

*** Corresponding Author**

Pr. Amélie BOCHOT: +33 1 46 86 55 79; amelie.bochot@universite-paris-saclay.fr

Abstract

Despite the high incidence of inner ear disorders, there are still no dedicated medications on the market. Drugs are currently administered by the intratympanic route, the safest way to maximize drug concentration in the inner ear. Nevertheless, therapeutic doses are ensured for only a few minutes/hours using drug solutions or suspensions. The passage through the middle ear barrier strongly depends on drug physicochemical characteristics. For the past 15 years, drug encapsulation into nanocarriers has been developed to overcome this drawback. Nanocarriers are well known to sustain drug release and protect it from degradation. In this review, *in vivo* studies are detailed concerning nanocarrier biodistribution, their pathway mechanisms in the inner ear and the resulting drug pharmacokinetics. Key parameters influencing nanocarrier biodistribution are identified and discussed: nanocarrier size, concentration, surface composition and shape. Recent advanced strategies that combine nanocarriers with hydrogels, specific tissue targeting or modification of the round window permeability (cell-penetrating peptide, magnetic delivery) are explored. Most of the

nanocarriers appear to be safe for the inner ear and provide a significant efficacy over classic formulations in animal models. However, many challenges remain to be overcome for future clinical applications.

Keywords

Cochlea, hydrogels, intracochlear administration, intratympanic administration, nanoparticulate systems, round window membrane, targeting

Abbreviations

C_{max}, maximum drug concentration achieved in perilymph; cryoTEM, transmission electron cryomicroscopy; ELISA, enzyme-linked immunosorbent assay; FDA, Food and Drug Administration; FITC, fluorescein isothiocyanate; GFP, green fluorescent protein; GJB2, gap junction protein beta 2; LC-MS, liquid chromatography-mass spectrometry; PdI, polydispersity index; PEG, poly(ethylene glycol); PLA, polylactic acid; PLGA, poly(lactic-co-glycolic acid); RT–PCR, reverse transcription–polymerase chain reaction; RWM, round window membrane; siRNA, small interfering RNA; SPION, superparamagnetic iron oxide nanoparticles; TEM, transmission electron microscopy; TRITC, tetramethylrhodamine; TTI, transtympanic injection

1. Introduction

More than 5% of the world's population has disabling hearing loss, and this may double by 2050 (World Health Organization, 2019). Hearing loss can be a consequence of several factors: noise exposure, aging, ototoxicity of drugs, autoimmune response or genetic impairment (Smouha, 2013). As auditory sensory cells do not regenerate (Schilder et al., 2019); hearing is restored by conventional hearing aids for mild and moderate hearing loss or cochlear implants for severe to profound sensorineural hearing loss (Roche and Hansen, 2015). Besides deafness or tinnitus, additional vestibular disorders (balance dysfunctions) may occur. Despite the high incidence of these diseases and their impact on quality-of-life, there is still no dedicated medication on the market and some drugs are used off-label.

The inner ear is a very isolated organ located in the temporal bone and protected by many physiological barriers (Nyberg et al., 2019). Over the last 30 years, the local administration of drugs has been developed to maximize drug diffusion into the inner ear (Plontke and Salt, 2018). Intratympanic administration by injection of the drug inside the middle ear cavity is a safe and common route of administration used in the clinic (Lechner et al., 2019). Currently, anti-inflammatory drugs are being evaluated on a wide range of inner ear diseases in clinical trials using intratympanic administration (Bento et al., 2016; Marshak et al., 2014; Patel, 2017; Santa Maria et al., 2013). Results

are partially mitigated because of the lack of efficient conventional dosage forms for the inner ear. Indeed, solutions and suspensions are rapidly eliminated by the Eustachian tube reducing the drug half-time in the cochlea. Repeated injections are then required, decreasing patient compliance. Currently, drugs from different therapeutic classes have emerged in clinical trials: antioxidants (Ebselen, Sound Pharmaceuticals), anti-inflammatory (Otividex®, Otonomy, Inc.), or anti-apoptotic drugs (D-c-Jun kinase inhibitor-1, Auris Medical) (Schilder et al., 2019). To give them a chance of success, there is an urgent need for efficient drug delivery systems for the inner ear (El Kechai et al., 2015a; Mäder et al., 2018).

Nanocarriers are nanoscale drug delivery systems (<1 µm) with tunable surface and physicochemical properties. Due to their numerous advantages, over the past 15 years, they have generated considerable interest for drug delivery to the inner ear (Mäder et al., 2018; Mittal et al., 2019). Nanocarriers may compensate drug properties such as low solubility, degradation, short half-life and low passage across physiological barriers. They may also offer the possibility to release the drug in a sustained manner and to address it to specific tissues (Agrahari et al., 2017). Several reviews have described the success of nanocarriers to treat or prevent inner ear diseases such as noise-induced hearing loss or drug ototoxicity (Kim, 2017; Li et al., 2017; Mittal et al., 2019; Pyykkö et al., 2016). However, the critical physicochemical characteristics influencing the biodistribution of nanocarriers in the inner ear are not well defined. Drug pharmacokinetics after nanocarrier administration have not been thoroughly compared among nanocarriers and with other formulations such as liquid forms or hydrogels.

This review focuses on nanocarrier characteristics leading to their improved efficacy against inner ear diseases. First, a brief overview of ear anatomy is presented, as well as the advantages of intratympanic administration. Second, the nanocarrier biodistribution, drug pharmacokinetics and key characteristics to deliver drugs from nanocarriers in the inner ear are presented. Then, we give an overview of the present and future advanced strategies to improve nanocarrier entrance into the inner ear. Finally, the safety and therapeutic efficacy of nanocarriers used in different inner ear disorders are discussed.

2. Anatomy and physiology of hearing and balance

The ear is anatomically divided into three parts: the outer, middle, and inner ear (Fig. 1A). The outer ear is represented by the auricle (visible part of the ear) and the external auditory canal, which is closed by the tympanic membrane. The role of the outer ear is to channel sound waves into the auditory canal to induce vibrations of the tympanic membrane (Hayes et al., 2013). This membrane is around 0.6 mm in thickness in humans and consists of three layers: an outer cutaneous layer, a core of connective tissue and an inner layer of mucus (Hentzer, 1969). Thus, it isolates the air-filled cavity of the middle ear from the environment. The middle ear contains the ossicular chain – the malleus, incus,

and stapes – that conducts sound waves from the tympanic membrane to the inner ear. The Eustachian tube ends in the nasopharynx. It maintains equal air pressure on both sides of the tympanic membrane while swallowing or yawning. The inner ear, also named the labyrinth, lies deep within the petrous portion of the temporal bone, the hardest bone in the human body (Fig. 1A).

The inner ear consists of two entangled organs: the vestibular apparatus, which is the organ of balance, and the cochlea, the organ of hearing (Fig. 1A). The vestibular apparatus contains three semi-circular canals oriented in three different spatial directions, and two membranous sacs, the utricle and saccule, responding to gravitational forces (Mazzoni, 1990). In the utricle and saccule, small calcite crystals called otoliths increase local shearing forces in response to slight displacements of the head, then stimulating the hair cells located underneath. The semi-circular canals hold the ampulla crest located in each canal and which is composed of the cupula (cap gel) and hair cells.

The cochlea is a long tube coiled around the modiolus comprising the cochlear nerve fibers (8^{th} pair of cranial nerves) (Sakamoto and Hiraumi, 2014). The spiral tube contains three internal compartments: the scala media, which is separated from the scala tympani by the basilar membrane and from scala vestibuli by Reissner's membrane (Fig. 1B). The scala tympani ends on the round window membrane, which separates the inner ear from the middle ear. The scala vestibuli ends on the oval window membrane, on which the stapes rests. Resting on the basilar membrane, the sensory inner hair cells of the organ of Corti respond to the wave stimuli and generate an action potential on nervous fibers, whereas the outer hair cells amplify the signal (Fig. 1B) (Corey et al., 2017). The bioelectrical signals are transmitted to the spiral ganglion neurons located in the bony spiral canal, and then conveyed to the brain, where they are interpreted as sounds. High frequency waves stimulate the basal part of the cochlea whereas low frequencies stimulate the apex (Sakamoto and Hiraumi, 2014).

Within the inner ear, two separate fluid-filled compartments are present, one inside the other: the scala media, filled with endolymph (~8 µL in guinea pigs or rats), contained within the bony labyrinth filled with perilymph (~70 µL) (Fig. 1B) (El Kechai et al., 2015a). These fluids are totally different in composition: the endolymph, a high K^+ fluid, bathes the apical ciliated part of the sensory cells, whereas the perilymph, a high Na^+ fluid, bathes their basolateral synaptic part (Wangemann and Marcus, 2017).

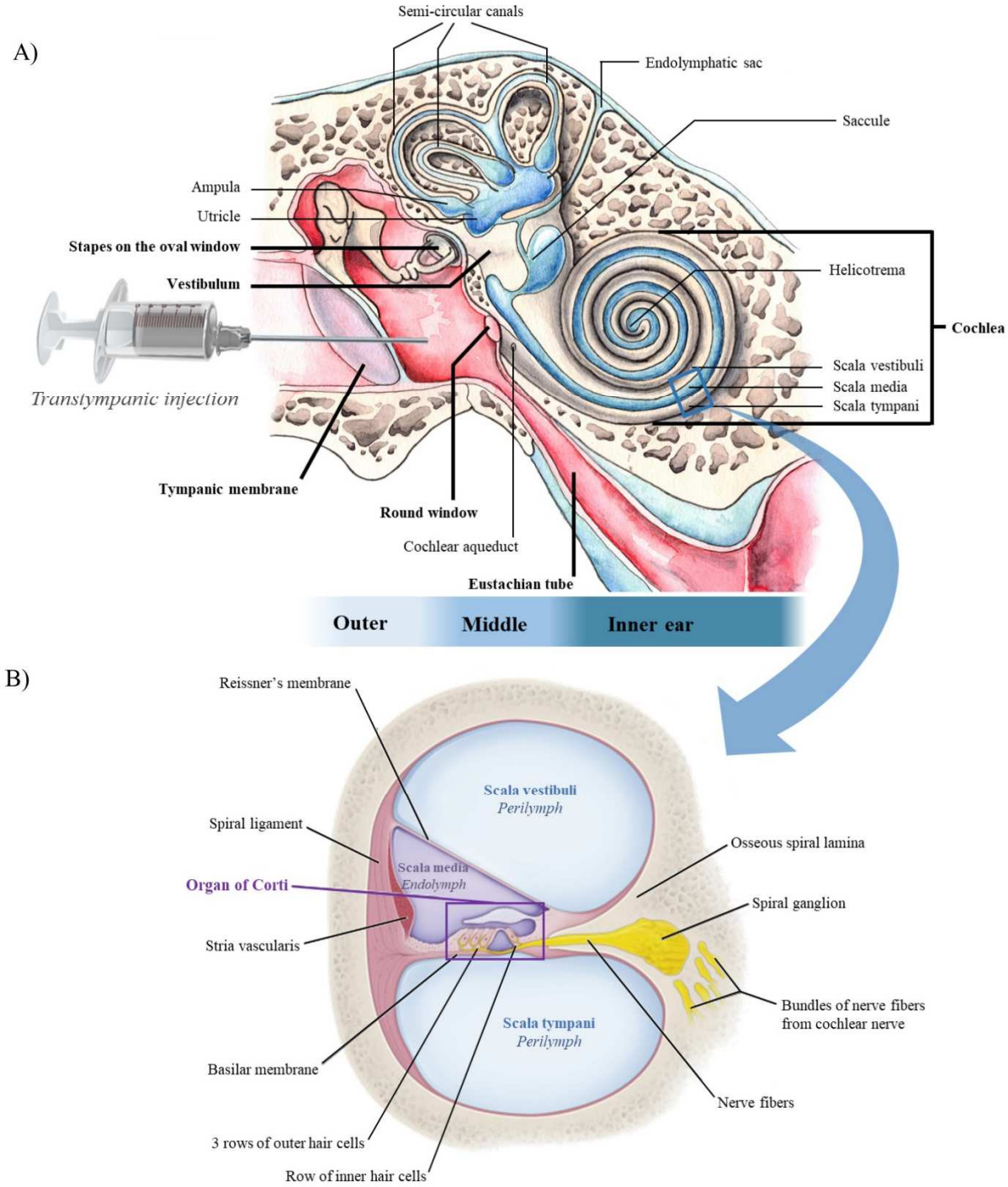

Fig. 1: A) Anatomy of the middle and inner ear, B) Anatomy of the cochlear canals.
B: reprinted from Maynard and Downes (2019) with permission from Elsevier.

3. Routes of administration for inner ear drug delivery

Several strategies of administration exist to deliver drugs to the inner ear: systemic access (oral or intravenous) and local administration (intracochlear or intratympanic). These routes are described in this section, with the different pharmaceutical forms used. Their advantages and limitations are detailed in Table 1.

3.1. Intravenous and oral administrations

In addition to common physiological barriers such as the hepatic passage or gut, drugs administered by intravenous and oral administration must cross the blood–labyrinth barrier to reach the inner ear. This barrier lies between the vasculature and inner ear fluids (perilymph and endolymph) (Nyberg et al., 2019) and dramatically restricts drug access to the inner ear. In the cochlea, the blood–labyrinth barrier is characterized by a continuous capillary endothelium with tight junctions (Jahnke, 1975; Juhn et al., 1981). The blood–endolymph barrier, localized within the stria vascularis, is even more complex: the tight junctions of the strial endothelium separate the lumen of the capillaries from the strial interstitial fluid, and a second epithelium separates the interstitial fluid from the endolymph compartment (Shi, 2016). Furthermore, exchanges between endolymph and perilymph are also restricted by the labyrinthine barrier. The presence of these barriers explains the limitations observed for drugs administered by these routes (Table 1).

Lipophilic and low molecular weight drugs are more susceptible to cross the blood–labyrinth barrier but the percentage of drug passage from the bloodstream is very low (around 0.000005% for methylprednisolone (Bird et al., 2007)). For some drugs, the blood–labyrinth barrier is even more selective than the blood–brain barrier. However, several conditions can influence the passage of drugs, including inflammation (Hirose et al., 2014; Zhang et al., 2015), diuretics (Liu et al., 2011), osmotic agents (Le and Blakley, 2017), elevated blood pressure (Inamura and Salt, 1992), and noise exposure in guinea pigs (Suzuki et al., 2002) but not in rats (Laurell et al., 2008).

3.2. Intracochlear administration

Intracochlear administration consists of the direct administration of the drug inside the cochlea (Table 1). Thus, there is no physiological barrier for the drug to access the inner ear. A small volume (a few microliters) of drug solution (Braun et al., 2011), suspension (Paasche et al., 2006) or gel (De Ceulaer et al., 2003), is slowly injected with a fine needle inside the cochlea through the round window membrane or by a cochleostomy. In the particular case of cochlear implantation, used to restore the hearing function in the case of severe to profound sensorineural hearing loss, drugs can be included within the coating (Richardson et al., 2009) or the silicone matrix of the electrode array (Douchement et al., 2015). Once placed in the scala tympani, the electrode array releases the drug in a sustained manner over several years. Unlike the simple intracochlear injection, this method is not used in humans at present. However, in the case of a drug-loaded electrode array, a long-term release in the perilymph would be obtained, which is not possible with intracochlear injection. Nevertheless, both techniques are extremely invasive and need a surgical approach under general anesthesia (El Kechai et al., 2015a). Because of its limitations (Table 1), intracochlear administration is not the most commonly used method of administration in clinical practice.

3.3. Intratympanic administration

The intratympanic route is the administration of a drug in the middle ear, and which must then dlipo This route offers many advantages over intracochlear administration (Table 1). The main technique used in clinical practice is transtympanic injection. The solution, suspension or hydrogel, is injected with a fine needle (~25 G) through the tympanic membrane, and fills the middle ear cavity (Liu et al., 2016). Then, the patient lies on the other ear for 15 to 30 minutes to maximize contact of the drug formulation with the round window membrane. Another route of intratympanic administration is the deposition of the solution only on the round window niche, using a sponge (Gelfoam®) or hydrogel to attain increased residence time in the middle ear. The application of Gelfoam® is not used by physicians to any great extent because it requires surgery to access the middle ear (Enticott et al., 2011). It has also been proposed to insert a wick through the tympanic membrane and place it in the round window region. The wick can be reloaded from ear drops administered to the external auditory canal (Silverstein et al., 2004).

Corticoids are mainly used in clinical practice (off-label) by transtympanic injection to treat sudden hearing loss (Lechner et al., 2019), Ménière's disease (Weckel et al., 2018) or to preserve hearing during cochlear implantation (Kuthubutheen et al., 2016). New therapeutics such as D-c-Jun kinase inhibitor-1 (AM-111, Auris Medical), peroxisome proliferator-activated receptor-γ agonist (STR001, Strekin AG), progenitor cell activator (FX-322, Frequency Therapeutics), and γ-secretase inhibitor (LY3056480, Audion Therapeutics) are currently in clinical trials for the treatment of sensorineural hearing loss (Schilder et al., 2019). Otonomy is developing a formulation containing gacyclidine (OTO-313) for the treatment of subjective tinnitus (phantom sounds only heard by the patient), and Synphora is testing an agonist of prostaglandin receptor, latanoprost (Xalatan®) for Ménière's disease (a disease associating vertigo, tinnitus, and low frequency hearing loss, with crisis evolution, linked to endolymphatic hydrops).

To reach the inner ear fluids, the drug must diffuse from the middle ear cavity through the round window and the oval window membranes, but also through areas of the otic capsule where the bone is thin in some animals, such as at the apex of the cochlea (Mikulec et al., 2009). Pharmacokinetics studies cannot be performed in humans. Perilymph sampling requires a highly invasive surgery under general anesthesia. The volume and pressure changes induced by the sampling of perilymph through the round window membrane can damage the fragile sensory epithelium of the cochlea, and thus induce non reversible profound hearing loss. However, in animals, it is possible to sample the perilymph to quantify the drug. The cochlea can also be collected, fixed and stained to assess the presence of drug. Knowing the dose administered in the middle ear, the amount of passage of the drug through the main local barriers (round and oval windows) can be quantified. The duration of drug release to the inner ear ranges from a few hours to a few days.

Table 1: Routes of administration to deliver drugs to the inner ear: benefits and limitations

Administration	Benefits	Limitations
Systemic or oral	- Easy to use in clinic with medical staff (intravenous) or without medical staff (oral)	- Blood–labyrinth barrier and temporal bone localization do not allow high molecular drug passage - Small lipophilic molecules only - Poor drug efficacy - Very low drug concentration in inner ear - High doses required - Huge systemic exposure leading to side effects
Intracochlear	- Minimized systemic exposure - Long-term local drug delivery possible (several weeks to years) - Avoid inner ear barriers, direct access to cochlea - Drugs can be delivered from electrode array coating - Adapted for liquid formulations and medical devices - Useful for safety evaluation and drug efficacy in preclinical studies	- Highly invasive - Small volume injected - Requires hospitalization and highly specialized medical staff - Potential toxicity of a high drug concentration in the cochlea - Risk of introducing pathogens in the inner ear - Risk of hearing trauma
Intratympanic	- Minimized systemic exposure - Short and middle term local drug delivery (several days to weeks) - Minimally invasive - Usually an outpatient procedure - Adapted for conventional liquid dosage forms, hydrogels, nanocarriers and medical devices - Repeated injections possible	- Requires diffusion through middle ear barriers to access the cochlea - High inter-individual variability (variable thickness of the round window, potential obstruction of the round window with false membranes) - Clearance of liquid formulations through the Eustachian tube - Risk of introducing pathogens in the middle ear - Risk of tympanic membrane perforation too large to heal

3.3.1. Round window membrane

The major barrier between the middle ear and the inner ear was long assumed to be the round window membrane (Goycoolea, 2001). It is located at the base of the cochlea, with regard to the scala tympani (Fig. 1A). The membrane consists of three layers: the outer epithelium facing the middle ear and comprising a single layer of cuboidal cells with microvilli. These cells are interconnected by tight junctions at the outer surface. The inner epithelium, bathing the perilymph, consists of squamous cells with large extracellular spaces (Goycoolea et al., 1988b; Goycoolea, 2001). These two layers are separated by a core of connective tissue made of collagen and elastic fibers that includes fibroblasts, lymphatic and blood vessels. When the middle ear is filled with aqueous content, the round window behaves like a semi-permeable membrane. Its permeability depends on several factors: duration of exposure, drug concentration, molar mass, liposolubility, electrical charge, thickness of the membrane and factors influencing its permeability (Goycoolea and Lundman, 1997) and using additives in the formulation composition such as benzyl alcohol (Mikulec et al., 2008).

- *Electrical charge*: cationic ferritin crosses easily through the outer layer of the membrane, carried by pinocytotic vesicles (Goycoolea et al., 1988a), whereas anionic ferritin is not able to pass through in rodents and cats (Goycoolea, 2001; Nomura, 1984).
- *Lipophilic* drugs are more likely to diffuse passively through the round window membrane compared to hydrophilic ones (Wang et al., 2011).

- *Drug molar mass*: low-molecular weight substances diffuse by paracellular pathways in the first layer of the round window membrane. Large substances follow specific transcellular pathways (Goycoolea, 2001). If such a specific pathway does not exist, the substance cannot reach the perilymph, as observed with albumin (70 kDa). Specific pathways can include receptor-mediated endocytosis, phagocytosis or channels between cells such as for latex spheres (Goycoolea et al., 1988b).
- The *average thickness of the round window* is 70 µm in humans (Goycoolea and Lundman, 1997) *versus* 10 to 14 µm in rodents (Goycoolea et al., 1988b). Thus, the barrier is more difficult to cross in humans than in rodents. However, the surface of the membrane is larger in humans (2.3 mm²; Okuno and Sando, 1988) than in guinea pigs (1.2 mm²; Ghiz et al., 2001).
- In *the presence of inflammation*, an increase in membrane permeability is observed in the early stages, but then the membrane becomes thicker and permeability decreases (Engmér et al., 2008).
- The entry of drugs into the human inner ear after intratympanic application may also be impeded by additional membranes or mucus (Engmér et al., 2008). Obstruction of the round window membrane with false membranes occurs in 33% of cases in humans (Alzamil and Linthicum, 2000).

3.3.2. Oval window membrane

Recently, the oval window has been demonstrated to be a substantial route of access for the inner ear. The amount of gadolinium-DOTA (~560 Da) able to enter the oval window in rats is 90% (Zou et al., 2012a). Amounts of drugs able to pass through the oval window are estimated at 35% against 65% for the round window membrane in guinea pigs, for both trimethylphenylammonium (~140 Da; Salt et al., 2012) and gentamicin (~480 Da; Salt et al., 2016).

Oval window is located at the beginning of scala vestibuli and is partly obstructed by the stapes, the base of which rests against the window (Fig. 1A). The stapes footplate is attached to the oval window by the annular ligament. This articulation is called the stapediovestibular joint. This joint is like every articulating surface, composed of a hyaline cartilage and a fluidic articular cavity, sealed by epithelial cells with tight junctions (Ohashi et al., 2008, 2006). The annular ligament has a porous structure, composed of a network of fibrillin, collagen and MAGP-36 (36 kDa microfibril-associated glycoprotein), the pores of which are filled with hyaluronic acid (Ohashi et al., 2008). Drugs with small molecular dimensions can diffuse through the annular ligament, which provides direct access to the perilymph, or even through the different layers of the oval window. The annular ligament thickness is variable in humans (0.26 to 0.64 mm) (Mohammadi et al., 2017) whereas it is fivefold thinner in rodents (Ohashi et al., 2008). Despite its possible advantages, the oval window pathway is rarely used.

3.3.3. Distribution and metabolism

The flow of inner ear fluids is very low, between 1.6 nL/min (Salt et al., 2015) and 30 nL/min (Ohyama et al., 1988) in guinea pigs (unknown in humans). Thus, the distribution of drugs, once in the perilymph, is mainly governed by passive diffusion, establishing a gradient from base to apex (Salt and Plontke, 2009). Drugs present in the scala tympani are distributed quickly into the spiral ligament, scala vestibuli and the vestibule. Therefore, the presence of the active substance in the vestibule does not necessarily indicate a passage through the oval window. The drug can also diffuse through the large pores of the osseous spiral lamina to spread into the modiolus (Rask-Andersen et al., 2006). In humans, the modiolar wall of the scala vestibuli and tympani is porous, composed of a web of connective tissue within the perilymph, forming a perilymphatic route to the modiolar space (Salt and Plontke, 2018). Diffusion to the endolymph is thought to depend on the charge of the molecule, because cationic markers, such as gadolinium-DOTA (Zou et al., 2012a), are excluded from the endolymph as Reissner's membrane is positively charged (+ 80 mV) (Nyberg et al., 2019).

Metabolism is sometimes crucial for drug efficacy (prodrugs) but can also lead to its rapid degradation. The perilymph contains proteins (2 mg/mL) and enzymes such as lactate dehydrogenase (Scheibe and Haupt, 1985), aminotransferases (Lysaght et al., 2011) and phosphodiesterases (Swan et al., 2009). For instance, dexamethasone phosphate (Hargunani et al., 2006) and triamcinolone acetonide (Salt and Plontke, 2018) are metabolized within the ear into their biologically active moieties by phosphodiesterases, but when administered into the middle ear, just a fraction of the total amount of drug is transformed (El Kechai et al., 2016; Salt and Plontke, 2018).

3.3.4. Elimination

Elimination of drugs starts in the middle ear: the Eustachian tube eliminates liquid forms in less than 30 minutes in humans (Plontke et al., 2008). In the inner ear, elimination is performed by two main pathways: the vascular system (Salt and Plontke, 2009) and the cochlear aqueduct (Salt and Plontke, 2018). As the vasculature of the inner ear is not directly in contact with the scalae, but is contained within the bony canals, direct elimination of drugs from the perilymph by blood vessels is unlikely (Salt and Plontke, 2009). However, it may occur after drug diffusion into the spiral ganglion, the organ of Corti or the lateral wall, for which fluid pathways exist from the perilymph to the blood vessels.

The cochlear aqueduct is a bony channel from the end of the cranium, connected to the scala tympani just next to the round window (Gopen et al., 1997; Salt and Hirose, 2018) (Fig. 1A). In rodents, this aqueduct allows fluid efflux (0.5–1 µL/min in guinea pigs) (Salt and Stopp, 1979), thus promoting drug diffusion into the cerebrospinal fluid (Salt and Hirose, 2018). Drugs can even be found in the brain after intratympanic administration and then in the contralateral ear (Chen et al., 2007; Zhang et al., 2013). The cochlear aqueduct in humans is longer, and exchanges between the perilymph and cerebrospinal fluid are more restricted, but the duct is often permeable (Gopen et al., 1997). The potential elimination by this pathway in humans remains uncertain.

3.3.5. Characteristics of formulations for transtympanic injection

Formulations injected into the middle ear must be sterile, nonpyrogenic, with an osmolarity around 300 mOsm/L to avoid perilymph leakage, without preservatives and with a physiological pH (7.38–7.42) (Ph. Eur. 10.2, 2020a, 2020b).

Solutions and suspensions are easily injectable into the middle ear, but are also quickly eliminated by the Eustachian tube, thus repeated injections are needed. For this purpose, hydrogels increasingly being developed to prolong the residence time of the drug in the middle ear (El Kechai et al., 2015a; Mäder et al., 2018). Shear-thinning hydrogels, based on hyaluronic acid, are attractive because their viscosity decreases under shear during injection and they are rapidly recovered once injected due to their non-thixotropic behavior. Two hyaluronic acid gels developed by Auris Medical are in clinical trials: Sonsuvi® (Suckfuell et al., 2014) for sensorineural hearing loss treatment and Keyzilen® (Van De Heyning et al., 2014) for tinnitus treatment.

Thermosensitive hydrogels (e.g. poloxamer, chitosan-glycerophosphate) are also interesting since they are easily injected as liquids at room temperature and turn into gels at body temperature. Two thermosensitive hydrogels are currently in clinical trials for treatment of sensorineural hearing loss (pioglitazone, Strekin AG) (Paciello et al., 2018) and Ménière's disease (OTOVIDEX®, Otonomy) (Otonomy, Inc., 2020).

4. Nanocarriers used in inner ear application

Drug delivery systems designed for intratympanic administration should meet the following specifications to be efficient (Mäder et al., 2018):

- Protect poorly sensitive drugs;
- Load a sufficient amount of drug to be efficient;
- Avoid rapid clearance by the Eustachian tube;
- Enable close contact with the round window membrane;
- Ensure effective transport of the drug through the round window membrane;
- Achieve a therapeutic dose in the inner ear;
- Target specific cells;
- Be safe.

Recently, approaches using nanocarriers have been proposed to overcome these hurdles. Nanocarriers are characterized by a diameter of less than 1 µm. They differ greatly with respect to the materials used (e.g. polymeric, lipid, inorganic), their size, surface charge, shape and biodegradability.

In the pharmaceutical field, nanocarriers provide many advantages in fighting cancer, pain management and antibiotic therapy (Gonçalves et al., 2020; Uchegbu and Siew, 2013). Indeed, due to their numerous advantages, they can compensate for disadvantageous drug properties such as low solubility, degradation, and short half-life. They can also sustain the release and provide high surface

exchange. Thus, nanocarriers for drug delivery to the inner ear have generated great interest over the last 15 years (El Kechai et al., 2015a; Mäder et al., 2018; Staecker and Rodgers, 2013). Polymeric nanoparticles, liposomes, polymersomes, cubosomes, lipid-based nanoparticles, dendrimer-based nanoparticles and superparamagnetic nanoparticles have been evaluated in preclinical studies for inner ear applications to administer small or macromolecules (Fig. 2).

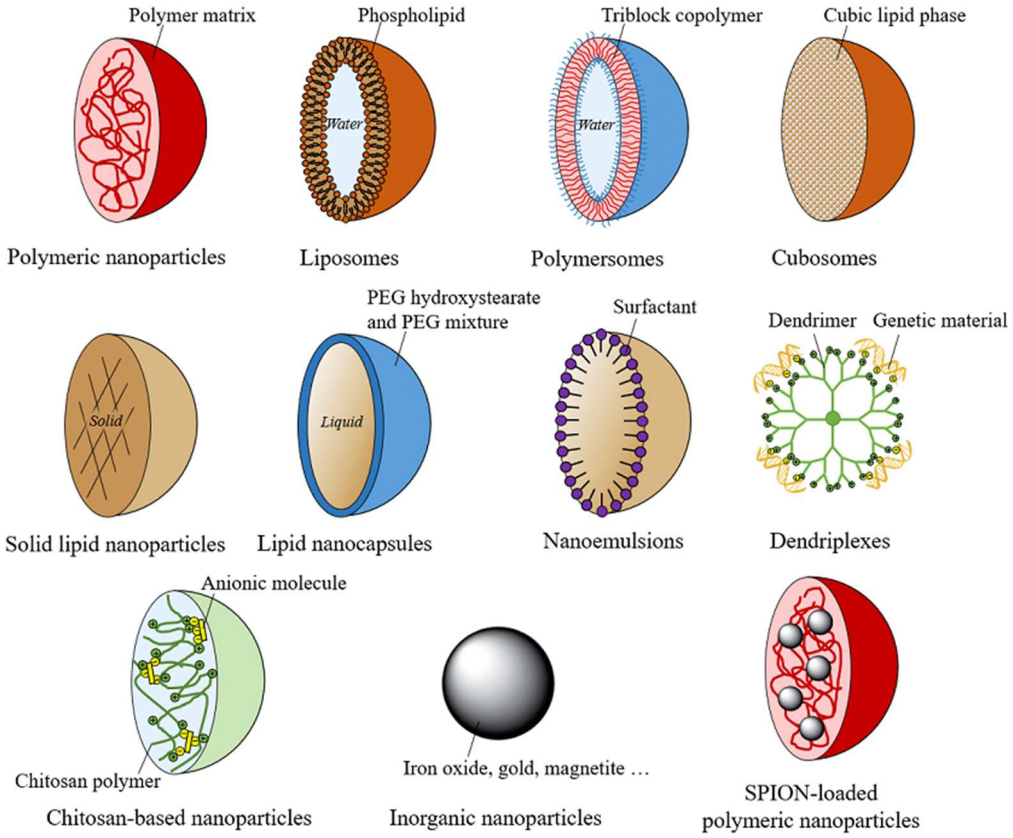

Fig. 2: Nanocarriers used for inner ear applications.
PEG, poly(ethylene glycol); SPION, superparamagnetic iron oxide nanoparticles.

Polymeric nanoparticles are mainly based on poly(lactic-co-glycolic acid) (PLGA), a biocompatible and biodegradable polymer approved by the Food and Drug Administration (FDA). Self-assembled polymeric nanoparticles obtained using drug-conjugated polymers are only tested in preclinical studies. They are based on copolymeric systems of *N*-vinylpyrrolidone and methacrylic derivatives conjugated to antioxidants (α-tocopherol, α-tocopheryl succinate) or anti-inflammatory drugs (ibuprofen) (Palao-Suay et al., 2015). These different types of polymeric nanoparticle allow the encapsulation of hydrophilic or lipophilic drugs in their polymeric matrix for inner ear delivery (see sections 5.1.3 and 7).

Liposomes are biocompatible vesicle-like lipidic nanocarriers, already on the market for other applications (Crommelin et al., 2020). Polymersomes have a similar structure, except that the outer shell is composed of self-assembled amphiphilic block copolymers instead of lipids (Chidanguro et al., 2018). In liposomes and polymersomes, hydrophilic drugs are encapsulated in the inner aqueous core and lipophilic drugs in the phospholipid bilayers or polymeric shell.

Cubosomes are nanocarriers formed from a lipid cubic phase and stabilized by a polymer (Barriga et al., 2019). The lipid cubic phase is a single lipid bilayer that forms a continuous porous structure containing aqueous medium. Compared to liposomes, the membrane surface area is more effective, allowing high drug loading of both hydrophilic (e.g. nerve growth factor) and lipophilic drugs.

Lipid-based nanocarriers allow the encapsulation of lipophilic drugs such as edaravone (antioxidant) or dexamethasone (anti-inflammatory drug) at higher drug loading (Nicolas and Vauthier, 2011). Solid lipid nanoparticles (solid core), lipid nanocapsules (liquid core) and nanoemulsions (stabilized oil nanodroplets dispersed in aqueous phase) have been described (Gao et al., 2015; Mohan et al., 2014; Yang et al., 2018).

Dendriplexes are composed of dendrimers, hyperbranched star-shaped macromolecules that exhibit hydrophobic cavities and a cationic surface. This cationic surface can bind to anionic nucleic acids and the hydrophobic regions to hydrophobic drugs (Wu et al., 2013).

Chitosan-based nanocarriers are stabilized by weak ionic interactions between chitosan and small anionic molecules (Vigani et al., 2019). They can encapsulate hydrophilic drugs in their gel-like matrix.

Inorganic nanoparticles are also used in biodistribution studies, because their material (maghemite, iron oxide or silver) is easily traceable by microtomography (Zou et al., 2015) or magnetic resonance imaging (Zou et al., 2010b, 2017b). Superparamagnetic iron oxide nanoparticles (SPION) are inorganic nanoparticles of small size (5–15 nm) that can be loaded into larger nanoparticles such as PLGA nanoparticles (Kopke et al., 2006) or chitosan nanocarriers (Ramaswamy et al., 2017). If an additional magnetic field is applied during the administration of the nanoparticles in the inner ear, the SPION are attracted and cross the round window membrane (see section 5.3).

All these nanocarriers have been studied to deliver either anti-inflammatory drugs (dexamethasone phosphate), antioxidants (edaravone) or antiapoptotic drugs (D-c-Jun kinase inhibitor-1) to protect the inner ear from noise exposure (Gao et al., 2015; Kayyali et al., 2018; Mamelle et al., 2018). Anti-inflammatory drugs (dexamethasone, methylprednisolone) and antioxidants (N-acetylcysteine, tocopheryl succinate) have also been tested to protect the inner ear against anticancer drug ototoxicity (Martín-Saldaña et al., 2018; Mohan et al., 2014; Sun et al., 2015; Wang et al., 2018). Finally, dexamethasone phosphate is also employed to reduce the trauma induced by cochlear implantation (Mamelle et al., 2017).

In the case of gene delivery to treat genetic hearing loss (Maeda et al., 2005), several nanocarriers have been evaluated: cationic liposomes, hyperbranched polylysine and dendriplexes. Nucleic acids (e.g. siRNA, mRNA), due to their negative charges bind to cationic charges at the surface of liposomes, to the cationic hyperbranched polylysine or to cationic dendrimers (Degors et al., 2019).

5. Nanocarrier biodistribution and pharmacokinetics

The efficacy of nanocarriers after intratympanic administration depends on their ability to accumulate inside the round window membrane or in the inner ear tissues and to release the drug to the perilymph. It raises several issues concerning their biodistribution and drug release in the inner ear. What is their fate after intratympanic administration? Do they enhance drug bioavailability? What are the key parameters influencing nanocarrier biodistribution and drug release? This section focuses first on nanocarrier biodistribution and drug pharmacokinetics after nanocarrier administration. The key physicochemical characteristics of nanocarriers for inner ear delivery are discussed. Finally, advanced approaches enhancing nanocarrier diffusion through the inner ear barriers are presented.

5.1. Passive approaches

Published studies on the biodistribution of nanocarriers and pharmacokinetics are summarized in Table 2. They were performed exclusively in rodents. Different types of nanocarrier were evaluated, based on polymer, lipid or iron with different surfaces (neutral, anionic, cationic or PEGylated). Many of the nanocarriers were PEGylated (Table 2). Nanocarrier size ranged from 10 to 630 nm but most of them had a diameter centered around 140 nm. *In vivo* studies were carried out over periods ranging from 2 hours to 2 weeks but most often over a short period (3 days).

To assess nanocarrier biodistribution, a fluorescent tracer can be covalently linked to the raw material of the nanocarrier or encapsulated inside it. Then the cochlea can be observed by confocal microscopy to track labeled nanocarriers (Table 2). However, when the tracer is not covalently bonded, it can be released from the nanocarrier depending on its characteristics. When fluorescent dots are observed in tissues, the tracer is probably still inside the nanocarrier whereas if the fluorescence is diffuse, then the probe has probably been released.

To evaluate drug pharmacokinetics, it is essential to have sensitive analytical techniques to quantify the drug in the perilymph. HPLC coupled to a UV or mass spectrometer (LC-MS) is generally used. However, when sampling the perilymph, small volumes (~2 µL) are taken to avoid contamination of the perilymph with cerebrospinal fluid. After sampling, the animal is euthanized, since multiple sampling is very difficult to set up (Salt and Plontke, 2018). Another approach is to label the cochlea by immunostaining specifically to detect the drug, or alternatively to develop high resolution imaging (Zou et al., 2016).

Table 2: Biodistribution of nanocarriers and pharmacokinetics after intratympanic administration

Nanocarrier	Nanocarrier characteristics	Drug/Tracer	Study design	Administration	Nanocarrier biodistribution and pharmacokinetics	Detection/ quantification method of the nanocarrier	Detection/ quantification method of the drug/tracer	Hypothesis on nanocarrier pathway mechanism	Reference
Liposomes									
Cationic liposome	ns	Plasmid leading to human GFP cell expression	Mouse n = 2/group 3 days	Sponge applied on RWM for 3 days	Gene expression in spiral ganglion, Reissner's membrane, organ of Corti, spiral limbus.		Fluorescence (not quantified)		(Jero et al., 2001b)
Cationic liposome	ns	Plasmid leading to GFP cell expression	Mouse n = 1/group 3 days	Sponge applied on RWM for 3 days	Gene expression in spiral ganglion, Reissner's membrane, spiral limbus, organ of Corti and vestibular hair cells. Higher expression at cochlea base.		Fluorescence (not quantified)	Cationic charge of liposomes may facilitate RWM passage.	(Jero et al., 2001a)
PEGylated liposomes	130 ± 20 nm	Gadolinium-DOTA	Rat n = 14 for the whole study 2 days	TTI	3 h after administration: gadolinium-DOTA detected in vestibule and first turn of cochlea. Detection in perilymph but not in endolymph compartment. 6 h: diffusion to second turn of cochlea. No more detection at day 1. 21% global passage of gadolinium-DOTA from middle ear to inner ear.		Magnetic resonance imaging (semi-quantified)	Main passage by oval window membrane.	(Zou et al., 2010a)
PEGylated liposomes	95 ± 10, 130 ± 10 and 240 ± 15 nm	Gadolinium-DOTA, TRITC-labeled	Rat n = 11/group 2 days	TTI	95 nm-liposomes observed in perilymph without loss of integrity. No more liposome detection at day 2. Gadolinium-DOTA transport in inner ear depends on liposome size: 95 nm > 130 nm > 240 nm Gadolinium-DOTA found mostly in ossicular chain, then in vestibule and scala vestibuli. Liposomes found 6 h after administration in utricle, spiral ligament and spiral ganglion.	Fluorescence (not quantified), cryoTEM on perilymph	Magnetic resonance imaging (semi-quantified)	Size-dependent passage. Both round and oval windows passage. Paracellular pathway.	(Zou et al., 2012b)
Cationic PEGylated liposomes	105 ± 15 nm PdI = 0.04 +14 mV	Gadolinium-DOTA or indocarbocyanine dye	Rat n = 14 for the whole study 1 day	Application on RWM or ossicular chain	For both application sites, gadolinium-DOTA detected in cochlea but not in the vestibule and in endolymph compartment. No more detection of gadolinium-DOTA at day 1. *RWM application:* Gadolinium-DOTA detected at 3 h, mainly in the RWM, with a decreasing gradient from basal to apex turns of the cochlea. *Ossicular chain application:* Gadolinium-DOTA detected in scala tympani at 3 h. Liposomes diffuse through the ossicular chain to reach both the oval and the round window membranes. Liposomes localized in the footplate, in nuclei and perinuclear region of the chondrocytes. No detection of liposomes in the annular ligament. Slight detection in the utricle of liposomes, that might diffuse from the cochlea.	Fluorescence (not quantified)	Magnetic resonance imaging (semi-quantified)	*RWM application:* accumulation of cationic PEGylated liposomes inside RWM. *Ossicular chain application:* cationic PEGylated liposomes do not cross oval window membrane. Accumulation of liposomes in the chondrocytes of the stapes.	(Zou et al., 2014b)

ns, not specified; cryoTEM, transmission electron cryomicroscopy; GFP, green fluorescent protein; PdI, polydispersity index; PEG, poly(ethylene glycol); RWM, round window membrane; TRITC, tetramethylrhodamine isothiocyanate; TTI, transtympanic injection.

Table 2: Biodistribution of nanocarriers and pharmacokinetics after intratympanic administration (continued)

Nanocarrier	Nanocarrier characteristics	Drug/Tracer	Study design	Administration	Nanocarrier biodistribution and pharmacokinetics	Detection/ quantification method of the nanocarrier	Detection/ quantification method of the drug/tracer	Hypothesis on nanocarrier pathway mechanism	Reference
Polymersomes									
PEGylated liposomes ***Versus*** **PEGylated polymersome**	82 nm, PdI = 0.05 90 nm	Rhodamine-lipid labeled, disulfiram (100 ng) Indocarbocyanine dye and disulfiram (100 ng)	Mouse n = 30 2 weeks	Sponge applied on RWM for 2 weeks.	Both nanocarriers found in the cytoplasm of the spiral ganglion neurons of each turn, hair cells, spiral ligament, stria vascularis, and in all layers of RWM at day 1. Same distribution for both nanocarriers but liposomes are present in higher number in spiral ganglion (45% *versus* 35% of neuron cytoplasms at day 2). High accumulation of polymersomes in RWM outer layer. Liposomes more efficient than polymersomes to deliver disulfiram.	Fluorescence (not quantified)	Disulfiram toxicity on hearing thresholds (quantified)	Liposomes cross RWM. They reach Rosenthal canal through the porous spiral lamina and spread to other turns of the cochlea. Polymersomes did not cross the RWM.	(Buckiová et al., 2012)
PEGylated polymersomes	83 ± 17 nm	Indocarbocyanine dye	Rat n = 16 for the whole study 3 to 5 days	TTI	Polymersomes accumulation in the outer layer of RWM. No polymersomes in connective tissue layer. Higher number of polymersomes in cochlea, 5 days after administration. Distribution in stria vascularis, basilar membrane, spiral ganglion and vestibule. No detection of polymersomes in endolymph.	Fluorescence (not quantified)			(Zhang et al., 2010)
PEGylated polymersomes	63 ± 10 nm	Indocarbocyanine dye	Rat n = 14 for the whole study 3 days	Sponge applied on RWM for 3 days or TTI	RWM: polymersomes only found in the outer layer. TTI induces 3-fold more polymersome passage in the inner ear than the sponge vehicle. Vestibule: TTI induces 2.5-fold more polymersome passage than with the sponge vehicle.	Fluorescence (semi-quantified)		Polymersomes failed to cross RWM outer layer. Effective transport through oval window with TTI.	(Y. Zhang et al., 2011b)
Poly(amino acid)-based polymersomes	27 ± 16 nm –35 mV	FITC-labeled and Nile red	Mouse n = 4/group 1 day	Sponge applied on RWM for 1 day	Few polymersomes nearby inner hair cells and supporting cells within the organ of Corti. Few polymersomes found in modiolus, without loss of integrity. Nile red released in inner hair cells, but not in supporting cells. Sparse fluorescence in modiolus.	Fluorescence (not quantified)	Fluorescence (not quantified)		(Kim et al., 2015)

FITC, fluorescein isothiocyanate; LC-MS, liquid chromatography-mass spectrometry; PdI, polydispersity index; PEG, poly(ethylene glycol); RWM, round window membrane; TTI, transtympanic injection.

Table 2: Biodistribution of nanocarriers and pharmacokinetics after intratympanic administration (continued)

Nanocarrier	Nanocarrier characteristics	Drug/Tracer	Study design	Administration	Nanocarrier biodistribution and pharmacokinetics	Detection/ quantification method of the nanocarrier	Detection/ quantification method of the drug/tracer	Hypothesis on nanocarrier pathway mechanism	Reference
Lipid-based nanocarriers									
PEGylated lipid nanocapsules	52 ± 5 nm –55 ± 7 mV	Indocarbocyanine dye or Nile red, rhodamine or FITC-lipid labeled	Rat n = 5/point 1 week	Sponge applied on RWM for 30 min	30 min: nanocapsules found in spiral ganglion and hair cells without loss of integrity. Nanocapsules that lose their integrity found in nerve fibers and lateral wall. 1 h: nanocapsules found in inner and outer hair cells without loss of integrity. Nanocapsules lose their integrity in nerve fibers of organ of Corti and spiral ligament. Day 1: nanocapsules found in the paracellular pathway of the outer layer of RWM, with a fraction that lost its integrity. Day 7: low detection of nanocapsules in spiral ganglion but high detection in hair cells and nerf fibers of organ of Corti.	Fluorescence (semi-quantified)		Paracellular pathway of lipid nanocapsules through RWM. Increasing the residence time of the sponge induces an increase in nanocarrier accumulation in RWM.	(Zou et al., 2008)
Lipid nanoemulsions: - **Cationic PEGylated** - **Cationic** - **Anionic** - **Neutral**	 280 nm 0 mV 225 nm +25 mV 211 nm –26 mV 190 nm –4 mV	Dexamethasone (4.2 µg) or Nile red	Mouse Number ns 3 days	TTI	24 h after administration: cationic PEGylated nanoemulsions found in inner hair cells (concentration 2-fold higher compared to Nile red solution and cationic, anionic and neutral nanoemulsions). Release of dexamethasone by cationic PEGylated nanoemulsions to the inner ear equivalent to the dexamethasone phosphate solution which is more concentrated (dose ≈ 150 µg).	Fluorescence (semi-quantified)	Dexamethasone immunostaining (semi-quantified)	PEGylation promotes the diffusion of nanocarriers across middle ear mucosa and inner ear barriers.	(Yang et al., 2018)
PLA or PLGA-based nanoparticles									
PLGA nanoparticles	140–180 nm	Rhodamine B	Guinea pig n = 4/group 1 day	Sponge applied on RWM for 1 day	Nanoparticles present in RWM and in round window niche. Nanoparticles mostly in the basal turn of cochlea, in scala tympani and basilar membrane.	Fluorescence (not quantified)			(Tamura et al., 2005)
PLGA nanoparticles	Labelled nanoparticles: 135 nm PdI = 0.17 Drug-loaded nanoparticles: 154 nm PdI = 0.01	Coumarin-6 or salvianolic acid B (2 mg), tanshinone IIA (0.1 mg), panax notoginsenoside (3 mg)	Guinea pig n = 168 for the whole study 4 days	RWM application	*Coumarin-6 released* in perilymph up to 6 h by the nanoparticles, C_{max} = 201 ng/mL *versus* 18 ng/mL for the coumarin-6 solution. *Multidrug release:* up to 16 h in perilymph, for drug solution and drug-loaded nanoparticles. C_{max} in perilymph for drugs-loaded PLGA nanoparticles *versus* drug solution: salvianolic acid (350 *versus* 680 µg/mL), tanshinone (10 *versus* 36 µg/mL), panax notoginsenoside (~1000 *versus* ~100 µg/mL for each metabolites)		UV-quantification of coumarin-6, HPLC-UV for the different drugs (quantified)	Bioadhesion of PLGA nanoparticles on the outer surface of the RWM.	(Cai et al., 2014)

ns, not specified; LC-MS, liquid chromatography-mass spectrometry; PdI, polydispersity index; PEG, poly(ethylene glycol); PLA, polylactic acid; PLGA, poly(lactic-co-glycolic acid); RWM, round window membrane; TTI, transtympanic injection.

Table 2: Biodistribution of nanocarriers and pharmacokinetics after intratympanic administration (continued)

Nanocarrier	Nanocarrier characteristics	Drug/Tracer	Study design	Administration	Nanocarrier biodistribution and pharmacokinetics	Detection/ quantification method of the nanocarrier	Detection/ quantification method of the drug/tracer	Hypothesis on nanocarrier pathway mechanism	Reference
PLGA nanoparticles: - **Uncoated** - **PEGylated** - **Poloxamer-coating** - **Chitosan-coating**	 158 nm PdI = 0.12 135 nm PdI = 0.17 170 nm PdI = 0.11 155 nm PdI = 0.3	Coumarin-6	Guinea pig Number ns 1 day	TTI	Coumarin-6 in: - Uncoated: very low signal in outer hair cells (1 arbitrary unit) - PEGylated: spiral ganglion, outer hair cells (1.25 arbitrary units), gradient from base to apex - Poloxamer-coating: spiral ganglion, outer hair cells (2 arbitrary units), stria vascularis, of the 3 turns - Chitosan-coating: spiral ganglion, spiral ligament, very low signal in outer hair cells (1 arbitrary unit)		Fluorescence (semi-quantified)	PLGA nanoparticle surface plays a key role. Hydrophilic coating prevents clearance from middle ear by the ciliated epithelia by blocking hydrophobic interactions. Poloxamer decreases micro-viscosity, creating pores in outer hair cells.	(Wen et al., 2016)
PLGA nanoparticles: - **Uncoated** - **PEGylated** - **Poloxamer-coating** - **Chitosan-coating**	PdI <2 84 ± 4, 155 ± 5 nm, 292 ± 15 nm –8 mV 135 ± 5 nm –12 mV 185 ± 10 nm –16 mV 170 ± 15 nm +18 mV	Indocarbocyanine dye	Guinea pig n = 3/point 1 day	TTI	*Effect of size:* 0.5 h: higher passage of 300 nm-nanoparticles in cochlea compared to 150 nm and 80 nm-sized nanoparticles. 24 h: same quantification for all. *Effect of surface:* 0.5 h: chitosan-coated nanoparticles passage in cochlea is 2-fold higher than other PLGA-nanoparticles. 24 h: passage in cochlea more important for poloxamer > PEGylated ≈ chitosan > uncoated nanoparticles.	Fluorescence (semi-quantified)		Size-dependent and hydrophilic-dependent pathway to cochlea.	(Cai et al., 2017)
PLGA nanoparticles	160 nm PdI = 0.19 –12 mV [PLGA] tested: 10, 30 and 90 mg/mL	Coumarin-6	Guinea pig 10 to 60 min n = 3/point	TTI for 10 to 60 min	Nanoparticles present in perilymph 30 min after TTI, without loss of integrity. Coumarin-6 intensity increases in RWM from 10 to 30 min, and then drops at 60 min. Raising the concentration of administered nanoparticles increases the amount of nanoparticles inside the RWM. Nanoparticles are internalized in lysosomes to be degraded but also transported by exocytosis out of the cells. *Specific pathway mechanisms involved:* macropinocytosis, caveolae-mediated endocytosis pathway, exocytosis mediated by endoplasmic reticulum, Golgi apparatus and recycling endosomes. *Pathway mechanisms not involved:* clathrin-mediated endocytosis, paracellular transport.	TEM on perilymph and RWM samples (not quantified), confocal imaging on RWM (not quantified), HPLC-fluorescence detector of coumarin-6 in perilymph (quantified)		Nanoparticles enter in the inner ear in a concentration-dependent manner. *Pathway involved:* macropinocytosis, caveolae-mediated endocytosis pathway, exocytosis mediated by endoplasmic reticulum, Golgi apparatus and recycling endosomes. *Pathway not involved:* clathrin-mediated endocytosis, paracellular transport.	(Zhang et al., 2018)

ns, not specified; PdI, polydispersity index; PEG, poly(ethylene glycol); PLGA, poly(lactic-co-glycolic acid); RWM, round window membrane; TEM, transmission electron microscopy; TTI, transtympanic injection.

Table 2: Biodistribution of nanocarriers and pharmacokinetics after intratympanic administration (continued)

Nanocarrier	Nanocarrier characteristics	Drug/Tracer	Study design	Administration	Nanocarrier biodistribution and pharmacokinetics	Detection/ quantification method of the nanocarrier	Detection/ quantification method of the drug/tracer	Hypothesis on nanocarrier pathway mechanism	Reference
PEGylated PLA nanoparticles	130 nm PdI = 0.1 –26 mV	Dexamethasone (50 µg) or coumarin-6	Guinea pig n = 3–5/point 1 h to 2 days	RWM application	1 h after RWM application: strong coumarin-6 detection in stria vascularis, organ of Corti, spiral ganglion in each cochlea turn. Higher dexamethasone concentration (from 8 500 ng/mL at 1 h to 300 ng/mL at 48 h) with nanoparticles compared with dexamethasone phosphate solution (13 000 ng/mL at 1 h to 850 ng/mL at 6 h).		LC-MS in perilymph (quantified), fluorescence (not quantified)	Rapid accumulation of coumarin-6 in organ of Corti suggesting easy passage of RWM.	(Sun et al., 2015)
Miscellaneous									
Oleic acid and poloxamer 407-coated iron oxide nanoparticles	12 ± 0.5 nm Neutral charge		Rat n = 23 for the whole study 1 week	Sponge applied on RWM for 1 week *Without magnet delivery*	Slight passage through the RWM after sponge application. Nanoparticles released in inner ear up to 3 days. Nanoparticles found only in perilymphatic space of the saccule.	Magnetic resonance imaging (semi-quantified), Prussian blue staining (not quantified)			(Zou et al., 2010b)
Polyvinyl-pyrrolidone stabilized silver nanoparticles	117 ± 24 nm –20 ± 9 mV		Rat n = 2/point 1 week	TTI	At 24 h, nanoparticles found in RWM, oval window and scala tympani. No more detection of nanoparticles in the inner ear at 1 week.	Micro-tomography (semi-quantified)		Nanocarrier entrance in inner ear by both oval and round window membranes.	(Zou et al., 2015)
Maghemite nanoparticles	50–60 nm +55 mV		Rat n = 6 for the whole study 2 weeks	TTI *Without magnet delivery*	High accumulation of nanoparticles in RWM and oval window up to day 14. High nanoparticle accumulation in the basal turn of cochlea and vestibule 3 h post-TTI, starting to decrease at 6 h. Only a few nanoparticles in scala media. Slight detection of nanoparticles at day 1.	Magnetic resonance imaging (semi-quantified), Maghemite staining of RWM and oval window (not quantified)		Accumulation and diffusion of nanoparticles in both oval and round window membranes.	(Zou et al., 2017b)
Cubic glyceryl monooleate-based cubosomes	211 ± 23 nm PdI = 0.18 –27 mV	FITC-labeled enzyme or octadecyl rhodamine B	Guinea pig n = 8 for the whole study 1 day	TTI	Cubosomes found in RWM and basal turn of scala tympani, 30 min after administration. Labeled enzyme found in perilymph up to 24 h with cubosomes and 12 h in solution. C_{max} = 4 µg/mL with cubosomes against 2 µg/mL with the enzyme solution.	Fluorescence (not quantified)	Fluorescence (quantified)	Cubosomes entrance in the inner ear by the RWM.	(Liu et al., 2013b)
Bovine serum albumin-loaded cubosomes	215 nm PdI = 0.08 –23 mV	Nerve-growth factor	Guinea pig Number ns 1 day	Sponge applied on RWM for 1 day	At 2 h, C_{max} = 13 ng/mL for cubosomes and 2 ng/mL for solution. No more nerve-growth factor in perilymph at 6 h.		ELISA test (quantified)		(Bu et al., 2015)
Bovine serum albumin - nanoparticles	636 nm +5 mV	Rhodamine B	Guinea pig n = 1 for the whole study 3 days	TTI	Nanoparticles adhere to the RWM surface. Rhodamine B seems to be more abundant in the inner ear with nanoparticles than with solution 3 days after administration.	Scanning electron microscopy of the RWM surface.	Fluorescence (not quantified)	Deposit of nanoparticles on the outer surface of the RWM.	(Yu et al., 2014)

ns, not specified; ELISA, enzyme-linked immunosorbent assay; PdI, polydispersity index; PEG, poly(ethylene glycol); PLA, polylactic acid; RWM, round window membrane; TTI, transtympanic injection.

Table 2: Biodistribution of nanocarriers and pharmacokinetics after intratympanic administration (continued)

Nanocarrier	Nanocarrier characteristics	Drug/Tracer	Study design	Administration	Nanocarrier biodistribution and pharmacokinetics	Detection/ quantification method of the nanocarrier	Detection/ quantification method of the drug/tracer	Hypothesis on nanocarrier pathway mechanism	Reference
Dendriplexes modified or not with cyclodextrins *versus* Polyethylen-imine /DNA polyplexes	132 ± 20 nm PdI = 0.15 +31 mV 300–600 nm	Plasmid containing Atoh1 and GFP gene	Rat n = 17 for the whole study 1 week	Sponge applied on RWM for 1 week	*Cyclodextrin modified dendriplexes:* 48% and 82% of, respectively inner and outer hair cells showed GFP expression. Atoh1 gene expressed in cochlea sensory epithelium. *Non-modified dendriplexes:* expression < 10% in hair cells. *Polyplexes:* expression < 1% in hair cells.		Fluorescence (semi-quantified), western blot and RT–PCR (not quantified)		(Wu et al., 2013)
Hyper-branched polylysine	73 nm PdI = 1.9	FITC-labeled	Rat n = 6 for the whole study 1 day	Sponge applied on RWM for 1 day	Distribution gradient through the 3 layers of RWM. Perinuclear and in vesicle localization in outer layer and connective tissue. Abundant nanocarriers in organ of Corti and spiral ligament, few in spiral ganglion.	Fluorescence (not quantified)		Outer layer of RWM: transport to nucleus *via* nucleolin binding at cell surface.	(W. Zhang et al., 2011)
Nanoparticles based on drug-conjugated polymer (tocopherol, tocopheryl succinate, ibuprofen)	128–175 nm	Coumarin-6	Rat n = 2/group 2h	TTI	At 2 h, nanoparticles based on tocopherol or tocopheryl succinate observed in inner and outer hair cells. Decreasing gradient from basal to apical turn. Nanoparticles based on tocopheryl succinate and ibuprofen found in organ of Corti. They lose their integrity because coumarin-6 is released.	Fluorescence (not quantified)			(Martín-Saldaña et al., 2018, 2017, 2016)

FITC, fluorescein isothiocyanate; GFP, green fluorescent protein; PdI, polydispersity index; RT–PCR, reverse transcription polymerase chain reaction; RWM, round window membrane; TTI, transtympanic injection.

5.1.1.Biodistribution

When evaluated, nanocarriers are seen inside the round window (Buckiová et al., 2012; Liu et al., 2013b; Tamura et al., 2005; Yu et al., 2014; Zhang et al., 2018; W. Zhang et al., 2011; Y. Zhang et al., 2011a; Zou et al., 2008) and/or the oval window membranes (Zou et al., 2014b, 2015, 2017b) (Table 2). Cubosomes, hyperbranched polylysine, PLGA nanoparticles and PEGylated liposomes are distributed in the three layers of the round window membrane suggesting that they might diffuse inside this barrier (Buckiová et al., 2012; Liu et al., 2013b; Zhang et al., 2018; W. Zhang et al., 2011). Conversely, PEGylated polymersomes are only found in the outer layer of the round window membrane, suggesting that they are not able to cross this barrier (Y. Zhang et al., 2011a; Zhang et al., 2010). Nevertheless, they are detected in the inner ear, but only after transtympanic injection (Zhang et al., 2010) and not after round window application (Y. Zhang et al., 2011a). Since the transtympanic administration involved two access routes to the inner ear, the round and the oval window membranes, the entrance of PEGylated polymersomes into the inner ear might be carried out partially by the oval window membrane. Conversely, when PEGylated liposomes are applied to the ossicular chain, they are internalized in chondrocytes and fail to cross the oval window membrane (Zou et al., 2014b). Thus, the properties of the nanocarriers (size, nature of the surface, rigidity, shape or lipophilicity) may influence their ability to cross the round and/or the oval window membranes (see section 5.2).

Different types of nanocarriers are found in the inner ear after administration: liposomes, polymersomes, lipid nanocapsules, PLGA nanoparticles, cubosomes, inorganic nanoparticles, and hyperbranched polylysine, showing that they are able to cross middle ear barriers (Table 2). However, the proportion of these nanocarriers in the inner ear is not known. Indeed, methods of quantification of the nanocarriers are difficult to set up because their concentration needs to be related for instance to an intensity of fluorescence. The concentration of the nanocarrier raw material is sometimes assessed for inorganic nanoparticles in the perilymph (Zou et al., 2010b, 2015, 2017b), but never related to a concentration of nanocarriers or a percentage of the initial amount of nanocarriers administered. Semi-quantification of labeled nanocarriers is done using confocal microscopy (El Kechai et al., 2016) or spectrofluorometry on the sampled perilymph (Kayyali et al., 2018). These methods are used for advanced strategies of administration (see section 5.3), but not for standard nanocarrier administrations (Table 2).

Nanocarriers are mostly observed in the cochlea (Table 2); however, the vestibule is not always evaluated. Most of them are found in the basal turn of the cochlea (Buckiová et al., 2012; Liu et al., 2013b; Martín-Saldaña et al., 2017; Tamura et al., 2005; Zou et al., 2017b) and, when evaluated, in the vestibule (Zhang et al., 2010; Y. Zhang et al., 2011a; Zou et al., 2010b, 2014b, 2017b). If the oval window membrane is involved, by direct application on the oval window membrane or by transtympanic injection, nanocarriers are present in the vestibule (Ding et al., 2019; Zou et al., 2014b). Thus, specific targeting of the vestibule might be possible, for example, to treat Ménière's disease.

When specific tissue biodistribution is assessed, nanocarriers are principally located in the spiral ganglion (Buckiová et al., 2012; W. Zhang et al., 2011; Zhang et al., 2010; Zou et al., 2008) and around hair cells of the organ of Corti (Buckiová et al., 2012; Kim et al., 2015; Martín-Saldaña et al., 2018, 2016; Yang et al., 2018; W. Zhang et al., 2011; Zou et al., 2008). They are also visualized in the spiral ligament and stria vascularis (Buckiová et al., 2012; Zhang et al., 2010; Zou et al., 2012b, 2008). Liposomes and lipid nanocapsules can also be distributed in nerve fibers or the auditory nerve (Buckiová et al., 2012; Zou et al., 2008), suggesting that they are able to spread in the modiolus to reach other turns of the cochlea. Surprisingly, SPION exhibit a contradictory behavior, by accumulating only in the perilymphatic space of the saccule in the vestibule (Zou et al., 2010b). In this study, SPION are administered in the middle ear without the application of a magnet, as described in section 5.3. They might use an unknown specific pathway mechanism that causes their entrapment in saccule hair cells. Dendriplexes also reach specific tissue such as the hair cells of the organ of Corti (Wu et al., 2013). Otherwise, nanocarriers without targeting ligands do not seem to target a specific inner ear tissue (Table 2).

The integrity of nanocarriers once in the inner ear has not been evaluated for some nanocarriers (lipid nanoemulsions, dendriplexes, cubosomes, hyperbranched polylysine, chitosan nanocarriers). Their integrity has been demonstrate for PEGylated nanocapsules (Zou et al., 2008) and polymersomes (Kim et al., 2015) in the organ of Corti, and PEGylated liposomes (Zou et al., 2012b) and PLGA nanoparticles in the perilymph (Zhang et al., 2018). However, nanocarriers seem to lose their integrity when found in the spiral ligament (Zou et al., 2012b, 2008) or the supporting cells (Kim et al., 2015).

Nanocarriers seem to cross the middle ear barriers quickly, since they are detected in the inner ear for less than 1 hour (Liu et al., 2013b; Zhang et al., 2018; Zou et al., 2008) up to 3 hours (Zou et al., 2014b, 2017b) after administration. For PLGA nanoparticles, the peak concentration in the round window membrane occurs 30 minutes after transtympanic injection.

The persistence of the nanocarriers in the inner ear tissues depends strongly on their nature (Table 2). Lipid nanocapsules remain in the inner ear for 1 week (Zou et al., 2008), unlike to silver nanoparticles which are eliminated in less than 6 hours (Zou et al., 2015) or to liposomes eliminated/degraded in less than 24 hours (Zou et al., 2012b).

Most of the nanocarriers cross the middle ear barriers quickly to reach the basal turn of the cochlea and the vestibule, without targeting a specific tissue. They do not lose their integrity once in the perilymph (Kim et al., 2015; Zhang et al., 2018; Zou et al., 2012b, 2008); however, little is known about the fraction of nanocarriers that effectively reach the inner ear. Further studies are needed to evaluate this essential parameter.

5.1.2. Hypothesis on pathway mechanisms

Nanocarriers seem to enter the inner ear by either the round window (Buckiová et al., 2012; Zou et al., 2008, 2014b) or the oval window (Y. Zhang et al., 2011b; Zou et al., 2010b, 2015, 2017b). The hypothetical mechanisms of entrance through the round window membrane are widely discussed in the literature (Mittal et al., 2019; Pritz et al., 2013), but there is no detailed description for the mechanisms of entrance through the oval window (Table 2).

Lipid nanocapsules of small size (~50 nm) are thought to cross the first layer of the round window membrane by a paracellular pathway (Fig. 3), because they are found in the inner ear within 30 minutes (Zou et al., 2008). However, tight junctions between cells of the first layer might impede this pathway for larger nanocarriers (~150 nm) such as PLGA nanoparticles, which cross the outer layer of the round window membrane by transcellular pathways (Fig. 3). Multiple mechanisms of cell internalization are involved (Zhang et al., 2018). PLGA nanoparticles around 200 nm diameter, are internalized in macropinosomes (0.5–10 µm) using the macropinocytosis pathway (Fig. 3). Smaller PLGA nanoparticles are endocytosed in caveosomes (50–80 nm) by caveolae-mediated endocytosis (Zhang et al., 2018). These pathways lead to internalization of the nanoparticles into endosomes and then lysosomes. Once in the lysosomes, nanoparticles are trapped, and this might lead to drug release from nanoparticles or to nanocarrier degradation (Fig. 3). However, exocytosis mediated by the Golgi apparatus and the endoplasmic reticulum is also observed. Early endosomes can be recycled, which leads to the discharge of PLGA nanoparticles in the extracellular matrix (Fig. 3). These transcellular pathways are also described in the inner epithelium of the round window membrane and some fibroblasts (Zhang et al., 2018).

The mechanisms involved in the transcellular transport of PLGA nanoparticles have not been described for other types of nanocarriers. Clathrin-mediated endocytosis is not involved in the uptake of PLGA nanoparticles in the outer epithelium of the round window membrane (Zhang et al., 2018), but it can be involved for other types of nanocarriers. Cationic material has been shown to be transported by pinocytotic vesicles (Goycoolea and Lundman, 1997), but this has not been clearly demonstrated for cationic dendriplexes (Wu et al., 2013) and cationic liposomes (Jero et al., 2001b, 2001a). As described by Zhang et al. (2018), nanocarriers can accumulate within the cells or the connective tissue of the round window membrane without reaching the scala tympani. Liposomes and polymersomes are highly accumulated, respectively, inside the connective tissue and the outer layer of the round window membrane (Buckiová et al., 2012; Zou et al., 2014b). The drug can be released from the nanocarrier accumulated in the round window membrane. Thus, this barrier might act as a drug reservoir, though this has only been is demonstrated for advanced systems combining hydrogels and liposomes (El Kechai et al., 2016) (see section 5.3).

Concerning access through the oval window, nanocarriers are supposed to cross by the stapediovestibular joint (Fig. 3). Inorganic nanoparticles are clearly visible inside the joint after transtympanic injection (Zou et al., 2015, 2017b). Conversely, liposomes are not observed inside the

joint, but are internalized by the chondrocytes (Zou et al., 2014b); however, they might release their content in the inner ear in a sustained manner from the oval window.

Further studies are needed to evaluate which pathways are involved in the transport of nanocarriers across the round and oval window membranes. One must consider that this is a dynamic mechanism, and thus, the time window for observation of the phenomena must be carefully chosen to avoid misleading conclusions.

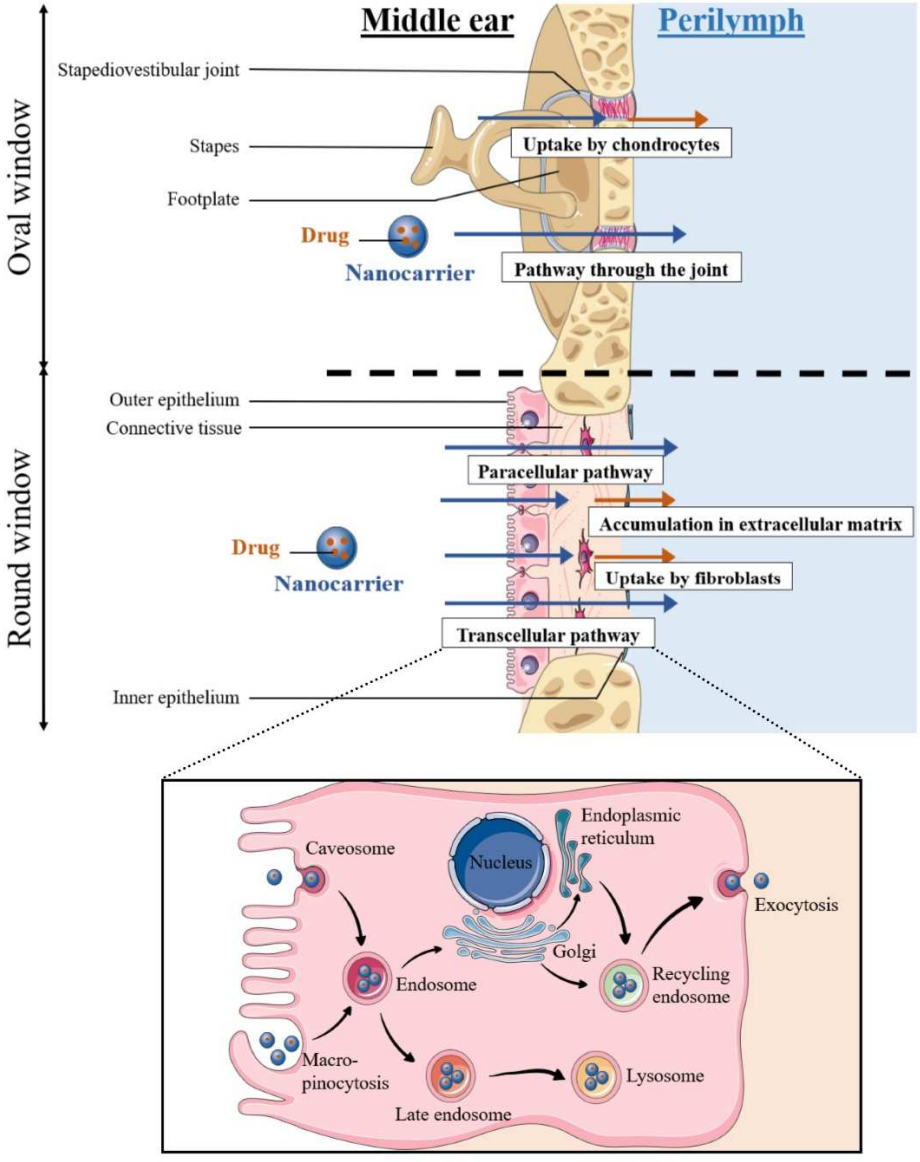

Fig. 3: Nanocarrier pathway mechanisms across middle ear barriers.

5.1.3. Pharmacokinetics

One of the goals of using nanocarriers is to increase the drug concentration in the inner ear to enhance drug efficacy. Compared to drug solutions, nanocarriers increase drug concentration and drug persistence in the inner ear in most of the studies (Bu et al., 2015; Cai et al., 2014; Liu et al., 2013a; Sun et al., 2015; Yang et al., 2018). For dexamethasone, therapeutic doses (30–40 ng/mL) (Kim et al., 2009) are reached with PEGylated PLGA nanoparticles and the delivery is extended from 12 to

48 hours compared to the solution (Sun et al., 2015). However, therapeutic doses are rarely documented for other drugs (*e.g.* nerve growth factor, salvianolic acid B, tanshinone IIA and panax notoginsenoside) (Table 2). Since the drug concentration and persistence are increased using nanocarriers, the drug entrance into the inner ear seems to rely on the characteristics of the nanocarrier and not of the drug; however, this is not always demonstrated. PLGA nanoparticles increase the concentration of a hydrophilic drug (panax notoginsenoside) in the perilymph compared to the drug solution, but not for lipophilic drugs (salvianolic acid B and tanshinone IIA) (Cai et al., 2014).

The biodistribution of nanocarriers and drug pharmacokinetics studies are rarely evaluated simultaneously (Table 2). When studied, the biodistribution of the nanocarrier seems to explain the kinetics of the active molecule. The nanocarrier concentrates the drug in its core, and then diffuses in the inner ear, which increases the drug concentration in the perilymph. For PLGA nanoparticles, the peak concentration of panax notoginsenoside observed around 30 to 60 minutes (Cai et al., 2014) is consistent with a rapid passage across the round window membrane (~30 minutes) (Zhang et al., 2018). For instance, PEGylated liposomes which can cross the round window membrane are more efficient in delivering disulfiram to the cochlea than polymersomes which are accumulated in the outer layer of the round window (Buckiová et al., 2012). Nevertheless, polymersomes are able to deliver disulfiram to the cochlea from this barrier which may act as a reservoir of polymersomes.

Despite its importance for drug activity, the stability of the drug is seldom documented. For gene delivery, the integrity of nucleic acids is particularly important for activity as this is easily degraded. This can be investigated by adding the green fluorescence protein gene to the vectorized plasmid. Thus, if a cell emits additional fluorescence at the specific wavelength of the green fluorescence protein, the gene must have been efficiently incorporated into its genome. After complexation with cationic liposomes (Jero et al., 2001a, 2001b) or dendriplexes (Wu et al., 2013), green fluorescence protein expression is observed in many cochlea tissues for cationic liposomes and in hair cells for dendriplexes (Table 2). Thus, cationic nanocarriers are efficient in delivering non-degraded macromolecules to the inner ear tissues, though their concentration has not been determined in these studies.

Another key point for drug activity is the conversion of the prodrug into its active form. Yet, some studies have not evaluated this point (Sun et al., 2015) due to the technical challenges related to the analytical method. However, it is important to evaluate for dexamethasone phosphate, which must be converted into dexamethasone to be active (see section 3.3.3). Polylactic acid nanoparticles (Sun et al., 2015) and nanoemulsions (Yang et al., 2018) encapsulated the active form of dexamethasone, but the control group received the prodrug dexamethasone phosphate. Yang et al. (2018) quantified the active form of dexamethasone in tissues and demonstrated that dexamethasone concentration is equivalent between groups (dexamethasone-loaded nanoemulsions *versus* dexamethasone phosphate). Thus, this point must be systematically evaluated.

To conclude, nanocarriers seem to improve the drug pharmacokinetics profile in terms of drug persistence and concentration in the inner ear. The nanocarrier can protect the drug (Wu et al., 2013), diffuse into the inner ear through the middle ear barriers and cause increased drug concentration in the perilymph or inner ear tissues. However, the impact on the therapeutic effect of the drug/nanocarrier degradation in the middle ear barriers is poorly documented. Systematic studies evaluating both the biodistribution of nanocarriers and pharmacokinetics should be carried out to demonstrate clearly whether the increase in drug concentration in the inner ear is the consequence of nanocarrier diffusion and accumulation in the inner ear or to nanocarrier accumulation in the round window membrane and drug release from this membrane.

5.2. Key physicochemical characteristics for inner ear delivery using nanocarriers

The key parameters influencing the biodistribution of nanocarriers in the inner ear are difficult to identify because only a few studies have evaluated their influence for the same nanocarrier (Table 2). The size, the nature of the surface, the rigidity, the shape of the nanocarrier or the lipophilicity of the material used to manufacture the nanocarriers might all play a role in nanocarrier biodistribution. To properly evaluate the effect of physiochemical characteristics on nanocarrier delivery to the inner ear, the parameters should be modified one by one, which is rarely the case.

5.2.1.Influence of size

Most nanocarriers have a diameter centered around 140 nm without any real justification. The size of nanocarriers strongly influences their passage in the inner ear. However, comparisons were only evaluated for liposomes and PLGA nanoparticles (Cai et al., 2017; Zou et al., 2012b, 2010a). Indeed, small liposomes (~95 nm hydrodynamic diameter) accumulate more easily in the inner ear compared to larger ones (~240 nm) (Zou et al., 2012b, 2010a). Larger liposomes might be too large to cross the round window membrane. Conversely, PLGA nanoparticles demonstrate the opposite behavior (Cai et al., 2017). Only 30 minutes after transtympanic injection, 300 nm-sized nanoparticles are found in the cochlea with higher fluorescence levels than for 150 and 80 nm nanoparticles. However, 1 day after administration, fluorescence levels in the cochlea are similar whatever the size of PLGA nanoparticles (Cai et al., 2017). Those results might be explained by the kinetics of entrance of nanocarriers depending on their size (Zhang et al., 2018).

Thus, the effect of size might differ according to the type of nanocarrier; however, for a given size, there is an effect of the nanocarrier material. For instance, the round window membrane behaves differently for polymersomes and liposomes despite their similar size (around 90 nm) and vesicular structure (Buckiová et al., 2012). Liposomes reach the inner ear whereas polymersomes are embedded inside the outer layer of the round window. Although other parameters are most likely to be involved, nanocarrier size should be further evaluated because it also strongly influences drug encapsulation, and consequently the dose administered.

5.2.2. Influence of surface composition

The surface properties of nanocarriers can be modified using an anionic or cationic material, or a polymeric hydrophilic coating, such as chitosan, PEG or poloxamer that provides steric protection and a hydrophilic surface to the nanocarrier.

Cationic charge seems to induce a higher accumulation of nanocarriers in the inner ear compared to neutral and anionic ones (Table 2). Cationic PLGA nanoparticles are distributed in the inner ear within 30 minutes even though 1 day after administration, fluorescence levels in the cochlea are equivalent between cationic and PEGylated PLGA nanoparticles (Cai et al., 2017). However, for nanoemulsions, the cationic charge of the droplets must be combined with PEGylation to permit the delivery of Nile red to the inner ear (Yang et al., 2018). The difference between these two studies, aside from the type of nanocarrier used, may be explained by the cationic chitosan layer coating the PLGA nanoparticles. Chitosan chains provide a supplementary steric protection and a hydrophilic surface to the nanoparticles that might also favor their biodistribution in the inner ear.

Hydrophilic polymeric coating might play an important role. Although PEGylation is often used, its role in the biodistribution is not always evaluated (Table 2). PEGylated PLGA nanoparticles are not more highly accumulated in the inner ear than uncoated or cationic ones (Cai et al., 2017), but they deliver coumarin-6 more efficiently into the cochlea (Wen et al., 2016). PEGylated PLGA nanoparticles may accumulate in the round window membrane and release their content from there, which can be interesting from a safety point of view (see section 6).

The coating of PLGA nanoparticles with poloxamer strongly improves the delivery of coumarin-6 compared to PEGylated, chitosan-coated or uncoated ones (Wen et al., 2016). These authors suggest that poloxamer adsorption at the surface prevents nanoparticle clearance from the middle ear by the ciliated epithelium. This polymer inhibits hydrophobic interactions, hinders clearance and promotes nanoparticle entrance into the inner ear. In addition, poloxamer chains can interact with cell membranes, decrease the microviscosity of cell membranes and lead to pore formation (Demina et al., 2005). These authors hypothesize that it permits a higher outer hair cell penetration (Wen et al., 2016) but the integrity of nanoparticles in the outer hair cells has not been proved. Furthermore, one must consider that the uncoated nanoparticles in that study are in fact covered by polyvinyl alcohol (hydrophilic polymer) during manufacturing, as highlighted by Albert et al. (2018). PEG or poloxamer may be more hydrophilic and/or provide more steric protection than polyvinyl alcohol leading to nanocarrier accumulation in the cochlea.

To summarize, coating of the nanocarrier by a hydrophilic polymer (chitosan, PEG or poloxamer) seems to favor the passage of the nanocarrier into the inner ear. Further studies are needed to evaluate the impact of the charge independently of any other parameters (size or polymer coating).

5.2.3. Influence of nanocarrier concentration

Raising the concentration of PLGA nanoparticles from 10 to 90 mg/mL in the administered suspension increases their concentration inside the round window membrane (Zhang et al., 2018). The variation of silver nanoparticle concentration from 37 to 370 mM leads to a higher concentration in the perilymph (Zou et al., 2015). However, these later nanoparticles induce a local inflammation that enhances the permeability of the round window membrane. Thus, it may not be related to the nanoparticle concentration alone. Nanocarrier concentration does not seem to influence the kinetics of entrance of nanocarriers through the middle ear barriers (Zhang et al., 2018; Zou et al., 2015). Further studies are needed to evaluate whether it can prolong their persistence in the inner ear.

5.2.4. Other parameters

Other parameters might have an impact on the biodistribution of nanocarriers in the inner ear, such as the rigidity or the shape of the nanocarrier. However, up to now, this has rarely been evaluated. We can hypothesize that liposomes, due to their aqueous content and flexible lipid bilayers, are more susceptible to deform, unlike rigid PLGA nanoparticles. This might explain the difference in biodistribution observed when changing their size (see section 5.2.1).

In other applications such as cancer, elongated nanoparticles are used to increase the surface of contact with membranes and improve the uptake in cells (Cong et al., 2018). Cubic cubosomes may migrate through the round window membrane due to their larger contact surface compared to spherical nanocarriers (Liu et al., 2013b). However, the shape parameter has not been thoroughly investigated, though it could be interesting to evaluate.

5.3. Advanced approaches

Advanced delivery approaches to the inner ear are defined here as the combination of nanocarriers with an additional strategy. The aim is either to enhance drug release or to limit off-target effects. Several strategies are used (Table 3):

- Incorporation of the nanocarrier into a hydrogel vehicle;
- Active targeting allowing specific tissue therapy and which could be useful in the future development of gene therapy;
- Increasing the permeability of the round window by chemical (cell-penetrating peptide) or physical (magnetic delivery, ultrasound) triggers.

Table 3: Advanced approaches for nanocarrier and drug delivery to the inner ear

Nanocarrier	Nanocarrier characteristics	Drug /Tracer	Study design	Administration	Nanocarrier biodistribution and pharmacokinetics	Detection/ quantification method of the nanocarrier	Detection/ quantification method of the drug	Reference
Hydrogels containing nanocarriers								
Chitosan gel containing PEGylated liposomes	160 nm PdI = 0.16	Carboxy-fluorescein, rhodamine-labeled lipid	Mouse Number ns 1 day	RWM application	Liposomes found in perilymph after liposomal gel application, 2-fold more than with liposome suspension. Liposomes found in organ of Corti, without loss of their integrity.	Fluorescence (semi-quantified)	Fluorescence (semi-quantified)	(Lajud et al., 2015)
Hyaluronic acid gel containing PEGylated liposomes	146 ± 50 nm PdI = 0.1 –29 mV	Dexamethasone phosphate (1.5 mg) or rhodamine-labeled lipid	Guinea pig n = 42 for the whole study 1 month	TTI	Liposome accumulation inside RWM at day 2, in the perinuclear region of fibroblasts. Low number of intact liposomes in perilymph at day 2 (0.00003% of initial lipid concentration administered). Dexamethasone and dexamethasone phosphate quantified in perilymph up to 1 month with the liposomal gel. Conversion of dexamethasone phosphate into dexamethasone: C_{max} (dexamethasone) of 833 ± 382 ng/mL with liposomal gel against 39 ± 23 ng/mL for gel only at day 15. Macroscopic gel persistence in middle ear up to 1 week.	Fluorescence (semi-quantified)	LC-MS on perilymph (quantified)	(El Kechai et al., 2016)
Chitosan gel containing anionic liposomes	280 nm PdI = 0.23 −18 mV	Lipiodol-iopamidol 49 mg/mL	Mouse Number ns 1 day	RWM application	Slight diffusion of lipiodol-iopamidol in scala tympani observed when using liposomal gel. Higher diffusion of free-iodine contrast agents in cochlea.		Micro-tomography (not quantified)	(Kayyali et al., 2017)
Chitosan gel containing PLGA nanoparticles	290 ± 2 nm PdI = 0.08	Interferon α-2b (0.12 µg)	Guinea pig n = 38/point 4 days	TTI	C_{max}: solution > nanoparticles > hydrogel > nanoparticle-loaded hydrogel, respectively 540 > 470 > 305 > 290 ng/mL Release up to 70 h and 36 h, respectively for the nanoparticle-loaded hydrogel and other formulations (solution, nanoparticles, hydrogel). Interferon mean residence time increased with nanoparticle-loaded hydrogel (23 h) compared to hydrogel (14 h) or nanoparticles alone (10 h).		ELISA (quantified)	(Dai et al., 2018)
Chitosan nanocarriers dispersed or not in poloxamer gel	153 nm PdI = 0.14 +22 mV	Nile red	Guinea pig n = 18 for the whole study 4 h	TTI, RWM or oval window application	*Suspension administered by TTI:* 3-fold more Nile red in vestibule than in cochlea. Accumulation in stria vascularis in the cochlea. Presence of nanoparticles in perinuclear and paracellular pathways in oval window. Nanocarriers observed in the outer layer of RWM. *RWM application of nanoparticle-loaded hydrogel:* 6 ng Nile red/g cochlear tissue. *Oval window application of nanocarrier-loaded hydrogel:* 12 ng Nile red/g cochlear tissue. High passage in the vestibule.	Fluorescence (semi-quantified)	HPLC-UV after tissue extraction (quantified)	(Ding et al., 2019)
Active targeting of nanocarriers								
PEGylated polymersomes coated with Tet1 peptide	105 ± 20 nm –1 mV	Indocarbocyanine dye	Rat n = 27 for the whole study 3 days	TTI	Both targeted and untargeted polymersomes found in RWM, spiral ligament, scala vestibuli and tympani and Reissner's membrane. No accumulation in cochlear nerve.	Fluorescence (not quantified)		(Zhang et al., 2012)

ns, not specified; C_{max}, maximum drug concentration achieved in perilymph; ELISA, enzyme-linked immunosorbent assay; LC-MS, liquid chromatography-mass spectrometry; PdI, polydispersity index; PEG, poly(ethylene glycol); PLGA, poly(lactic-co-glycolic acid); RWM, round window membrane; TTI, transtympanic injection.

675

Table 3: Advanced approaches for nanocarrier and drug delivery to the inner ear (continued)

Nanocarrier	Nanocarrier characteristics	Drug /Tracer	Study design	Administration	Nanocarrier biodistribution and pharmacokinetics	Detection/ quantification method of the nanocarrier	Detection/ quantification method of the drug	Reference
PEGylated PLA nanoparticles coated with A666 peptide	157 ± 16 nm PdI = 0.1 –30 mV	Coumarin-6 or dexamethasone (0.7 µg)	Guinea pig n = 6 for the whole study 2 h to 2 days	RWM application	2 h after application, coumarin-6 found in the perinuclear region of outer hair cells and in modiolus, to a greater extent for targeted nanoparticles than for untargeted ones. Nevertheless, dexamethasone releases are not significantly different between A666-covered and untargeted PEGylated PLA nanoparticles with, respectively 295 and 444 ng/mL in perilymph 2 days after administration.		Fluorescence (not quantified) LC-MS for dexamethasone concentration in perilymph (quantified)	(Wang et al., 2018)
Chitosan gel containing PEGylated liposomes coated with prestin-targeting peptide-1	87 ± 5 nm	Plasmid encoding TdTomato and carboxy-fluorescein, rhodamine or cyanine 5-labeled lipid	Mouse n = 10/group 2 to 5 days	RWM application	5% of the targeted liposomes contained in the liposomal gel found in perilymph at day 2 (50 nM). Both targeted and untargeted liposomes found in outer hair cells of mid and basal turns of cochlea. Targeted liposomes reached the apical turn unlike untargeted ones. Both TdTomato and carboxyfluorescein are expressed by outer hair cells, but also in other tissues, after application of the gel containing targeted liposomes.	Fluorescence in perilymph sample (quantified)	Fluorescence (not quantified)	(Kayyali et al., 2018)
Cell-penetrating peptides								
Poly(amino acid)-based polymersomes coated with oligoarginine peptide	103 nm +22 mV	Nile red or GFP gene	Mouse Number ns 1 to 2 days	Sponge applied on RWM for 1 to 2 days	Gene expression found in modiolus and lateral wall at, respectively 1 and 2 days after administration. Nanoparticles found in organ of Corti, modiolus, and lateral wall. Loss of nanoparticle integrity for a fraction of the nanoparticles administered.		Fluorescence and GFP immunostaining (not quantified)	(Yoon et al., 2015)
PLGA nanoparticles - **Uncoated** - **Poloxamer coating** **Nanoparticles mixed or not with low molecular weight protamine**	PdI <2 155 ± 5 nm –13 mV 185 ± 10 nm –16 mV	Indocarbocyanine dye or coumarin-6	Guinea pig n = 3/point 1 day	TTI	Low molecular weight protamine increases nanoparticle passage in cochlear tissue. Both uncoated and poloxamer-coated nanoparticles found in spiral ganglion and stria vascularis, but also in organ of Corti for poloxamer-coated nanoparticles. Low molecular weight protamine increases the release of coumarin-6 in perilymph from 4 to 6 h for uncoated and poloxamer-coated nanoparticles.	Fluorescence (quantified)	HPLC-fluorescence detector (quantified)	(Cai et al., 2017)
Magnetic delivery								
PLGA nanoparticles containing oleic acid-coated SPION	180 nm PdI = 0.1		Rat n = 8 Guinea pig n = 3 Fresh human temporal bone n = 2 1 h	RWM application ± magnet	Nanoparticles that kept their integrity found in perilymph after magnetic field application: 51 ± 13 nanoparticles/µm² of TEM images. 2 nanoparticles/µm² of TEM images without magnetic field. Channel of nanoparticles visible in human RWM and presence of nanocarriers in perilymph.	TEM on perilymph samples and RWM (semi-quantified)		(Kopke et al., 2006)

ns, not specified; GFP, green fluorescent protein; LC-MS, liquid chromatography-mass spectrometry; PdI, polydispersity index; PEG, poly(ethylene glycol); PLGA, poly(lactic-co-glycolic acid); PLA, polylactic acid; RWM, round window membrane; SPION, superparamagnetic iron oxide nanoparticles; TEM, transmission electron microscopy; TTI, transtympanic injection.

Table 3: Advanced approaches for nanocarrier and drug delivery to the inner ear (continued)

Nanocarrier	Nanocarrier characteristics	Drug /Tracer	Study design	Administration	Nanocarrier biodistribution and pharmacokinetics	Detection/ quantification method of the nanocarrier	Detection/ quantification method of the drug	Reference
PLGA nanoparticles containing SPION	160–280 nm –20 mV		Chinchilla n = 3/group 40 min	TTI ± magnet	PLGA nanoparticle clusters found with or without exposure to magnetic field in spiral ligament, perilymph, Reissner's membrane, spiral ligament, stria vascularis, hair cells and RWM. Pinocytosis observed in RWM for large clusters.	TEM (not quantified)		(Ge et al., 2007)
PLGA nanoparticles containing SPION	483 ± 158 nm –20 mV	Dexamethasone acetate (0.8 µg)	Guinea pig n = 24 for the whole study 1 h	RWM application ± magnet	2-fold increase in dexamethasone concentration in cochlea (soft tissue, RWM, perilymph) using the magnetic field: 90 ng quantified/cochlea, 18 µg/mL in perilymph. 10% of the initial dose delivered in 60 min.		HPLC-UV (quantified)	(Du et al., 2013)
SPION dispersed in a hyaluronic acid gel	135 ± 5 nm		Rat n = 6 for the whole study 1 month	RWM application + magnet	High deposition of SPION in the first turn of scala tympani. SPION reached the second and third turns of cochlea. SPION present in organ of Corti, stria vascularis, spiral ganglion and modiolus. Nanoparticle-loaded hydrogel still present as a layer at the surface of the round window membrane.	Prussian blue staining (not quantified)		(Leterme et al., 2019)

PLGA, poly(lactic-co-glycolic acid); RWM, round window membrane; SPION, superparamagnetic iron oxide nanoparticles; TEM, transmi**ssion** electron microscopy; TTI, transtympanic injection.

5.3.1.Nanocarrier-loaded hydrogels

Over the past 5 years, hybrid systems combining nanocarriers and hydrogels have been increasingly developed for inner ear drug delivery (Table 3). Unlike sponges, hydrogels fill the whole cavity of the middle ear and their high viscosity reduces the elimination of nanocarriers by the Eustachian tube.

Three polymers are used as a matrix for nanocarrier administration: chitosan-glycerophosphate thermosensitive gel, poloxamer 407 thermosensitive gel and the shear-thinning non-thixotropic hyaluronic acid gel. They are combined with nanocarriers of different sizes (between 146 and 290 nm), different natures (PLGA nanoparticles, chitosan-based or liposomes) or different surfaces (PEGylated, cationic, anionic or neutral) (Table 3).

The incorporation of nanocarriers inside a hydrogel prolongs the drug residence time in the middle ear which increases the drug concentration in the perilymph compared to the drug-loaded hydrogel (Ding et al., 2019; El Kechai et al., 2016; Lajud et al., 2015). When the drug concentration in the perilymph is not enhanced by the hydrogel, the mean residence time of the drug in the inner ear is extended (Dai et al., 2018) (Table 3). Using this strategy, the sustained release of dexamethasone phosphate converted *in vivo* into dexamethasone (El Kechai et al., 2016) and interferon-α (Dai et al., 2018) occurs over 1 month and 3 days, respectively.

However, the increase in residence time of the hybrid hydrogel in the middle ear does not always improve inner ear exposure to the drug (Kayyali et al., 2017). In this study, the liposomes are quite large (280 nm hydrodynamic diameter) and the attractive interactions between the cationic chitosan polymer and the anionic liposomes might impede their diffusion inside the hydrogel or induce their destabilization (Kayyali et al., 2017).

If the nanocarriers do not retain their integrity after incorporation in the hydrogel, then they do not provide any protection or sustained release of the drug. Chitosan-glycerophosphate gel exhibits a macroporous microstructure, with well-interconnected pores (Dai et al., 2018; Qu et al., 2019). This gel microstructure does not change with anionic liposomes of 240 nm (Qu et al., 2019) or PLGA nanoparticles of 290 nm (Dai et al., 2018), though the gel has increased roughness. However, PEGylated liposomes of 160 nm lead to a “patchy” microstructure. If anionic liposomes (Kayyali et al., 2017) or PLGA nanoparticles (Dai et al., 2018) retain their integrity when incorporated into chitosan gels, this has not been demonstrated for PEGylated liposomes (Lajud et al., 2015). Nevertheless, PEGylation provides steric protection and hydrophilic surface for the liposomes incorporated in the chitosan hydrogel, preventing liposome destabilization. For hyaluronic acid and PEGylated liposome mixtures, clusters of intact but deformed liposomes are observed (El Kechai et al., 2015b). Poloxamer 407 is organized in a cubic micellar phase that drastically increases the viscosity of the medium (Dumortier et al., 2006) whereas weak ionic interactions are involved in the

formation of chitosan-based nanocarriers (Ding et al., 2019). Thus, assessing their integrity within the poloxamer gel is important.

If the liposomes can diffuse within the gel, they might be able to accumulate in the round window membrane and/or to diffuse into the inner ear, which can be an additional benefit of the system. This depends strongly on the electrostatic and steric interactions between the nanocarrier and the polymer network. PEGylated liposomes migrate from the gel towards the round window membrane (El Kechai et al., 2017). PEGylation provides steric protection to the liposomes and the anionic charges of these vesicles induce repulsive electrostatic interactions with the anionic polymer chains. In addition, the bicontinuous microstructure observed with this system also favors the long-distance migration of liposomes.

Little is known about the integrity of the nanocarriers once they have reached the inner ear. El Kechai et al. (2016) quantified the passage in perilymph of liposomes included in a hyaluronic acid gel which filled the middle ear. Despite the high lipidic concentration administered (40- to 80-fold more concentrated than other studies using liposomes), a very low amount of liposomes is detected in the perilymph (0.00003%). However, they are found internalized in the cytoplasm of cells in the round window membrane suggesting that this barrier acts like a reservoir of liposomes (El Kechai et al., 2016). It allows the sustained release of dexamethasone phosphate in the inner ear over 1 month. In another study, intact liposomes are found in the organ of Corti (Lajud et al., 2015). However, their concentration has not been determined (Table 3). The use of hydrogels combined with nanocarriers seems to be a very promising strategy to sustain drug delivery to the inner ear.

5.3.2.Active targeting to specific inner ear tissues

Active targeting allows drug delivery to specific tissues, reducing off-target effects. The ligand covalently fixed to the surface of the nanocarrier binds to a specific receptor present only on the targeted cells. In the inner ear application, effective targeting is first verified by intracochlear administration. Then, intratympanic administration is performed to evaluate *1)* the nanocarrier delivery to the cochlea and *2)* the accumulation of the nanocarriers in targeted tissues. Two main tissues are targeted: outer hair cells and spiral ganglion neurons.

- *Outer hair cell targeting*

The loss of outer hair cells leads to significant hearing loss (Dallos, 2008). The objective of therapeutics is to preserve outer hair cell survival to prevent noise or age-related sensorineural hearing loss. Two peptides have been developed, A665 and A666 peptides, to target the extracellular domain of prestin receptor, exclusively present on outer hair cell membrane (Dallos, 2008; Surovtseva et al., 2012). A666-PEGylated PLA (polylactic acid) nanoparticles lead to a specific release to the outer hair cells (Wang et al., 2018) but A665-gold nanoparticles do not (Kayyali et al., 2017). The absence of specific targeting can be due to a dissociation of the ligand from the nanoparticles inside the round window membrane (Kayyali et al., 2017). A modified A665 peptide, called Prestin-Targeting-Peptide-

1, is more efficient in targeting the outer hair cells (Kayyali et al., 2018); 5% of the initially administered targeted PEGylated liposomes are quantified in the perilymph 2 days after administration with the thermosensitive chitosan gel (Table 3). Targeted liposomes reach the apical turn of the cochlea while untargeted ones do not. Incorporation of the nanocarriers in the chitosan hydrogel does not impede their migration into the inner ear. After incorporation of a plasmid inside the liposomes, gene expression is achieved in outer hair cells but only with targeted liposomes (Kayyali et al., 2018). Thus, the liposomes seem to retain their integrity once in the inner ear. Although it was not discussed by the authors, targeted liposomes are also localized in off-target tissues (Kayyali et al., 2018). When loaded with c-Jun-N-terminal kinase inhibitor, a significant protection of hearing function is achieved with Prestin-Targeting-Peptide-1-coated liposomes compared to non-targeted ones (see section 7).

Thus, Prestin-Targeting-Peptide-1 seems to be the most efficient ligand to target outer hair cells. As the loss of activity of prestin in outer hair cells can lead to deafness (Dallos, 2008), the toxicity of this ligand should be evaluated.

- *Spiral ganglion neuron targeting*

Maintaining the survival of the spiral ganglion neurons significantly enhances cochlear implantation outcomes (Ramekers et al., 2015). In preclinical studies, neurotrophins (neuronal growth factors) efficiently improve neuronal density in the spiral ganglion and hearing thresholds (Kandathil et al., 2016). However, these drugs need to be continuously delivered, otherwise the benefit is lost (Shepherd et al., 2008).

A 13-mer Tet1 peptide is used to target the trisialoganglioside clostridial toxin receptor expressed in spiral ganglion neurons (Santi et al., 1994). This peptide specifically binds to this receptor and allows efficient targeting of brain neurons (Park et al., 2007). When conjugated to PEGylated polymersomes (Zhang et al., 2012), efficient targeting of the cochlear nerve and spiral ganglion neurons is achieved only by intracochlear administration. Intratympanic administration leads to biodistribution of polymersomes in the cochlea but not restricted to the neurons.

The discovery of new targets in other cell populations, such as the inner hair cells or supporting cells, to induce specific regeneration, could be interesting strategies in the future (Zhong et al., 2019).

5.3.3. Cell-penetrating peptides

Cell-penetrating peptides are composed of 6 to 30 amino acid residues able to increase cellular internalization and penetration in physiological barriers such as the blood–brain barrier (Silva et al., 2019). In preclinical studies, cell-penetrating peptides promote siRNA (Qi et al., 2014) and protein (Kashio et al., 2012; Takeda et al., 2016) delivery to the inner ear. Thus, combining cell-penetrating peptides with nanocarriers, either linked to their surface (Yoon et al., 2015) or mixed with the nanocarrier suspension (Cai et al., 2017), should enhance the passage of nanocarriers through the

round window membrane. Currently, two peptides have been reported: oligoarginine, a cationic 8-mer peptide, and low molecular weight protamine (Table 3).

When polymersomes are covered with oligoarginine (Yoon et al., 2015), the release of Nile red is more visible on confocal microscopy than for uncovered polymersomes in the organ of Corti (Kim et al., 2015). However, no quantification was performed in this study. Regarding low molecular weight protamine, it enhances the entrance of PLGA nanoparticles by the round window (Cai et al., 2017). The concentration of coumarin-6 in the inner ear is slightly increased by the presence of the cell-penetrating peptide on the surface of PLGA nanoparticles (Table 3).

5.3.4.Magnetic delivery of nanocarriers in the inner ear

The magnetic delivery of nanocarriers consists of the injection into the middle ear of SPION (5–15 nm), incorporated or not in a larger nanocarrier, that cross the round window membrane thanks to the application of a magnetic field (Kopke et al., 2006).

First, the proof-of-concept was established in guinea pigs and fresh human explants (Kopke et al., 2006). PLGA nanoparticles containing SPION were efficiently pulled from the middle to the inner ear by a magnet applied on the contralateral ear for 1 hour. A channel of nanoparticles was observed inside the round window membrane and a large amount of nanoparticles was found in the perilymph (Table 3). When dexamethasone acetate was incorporated into 500 nm-large PLGA nanoparticles, 10% of the initial dose applied to the round window membrane was quantified in the cochlea within 1 hour (Du et al., 2013). A very high dexamethasone concentration of 18 µg/mL was reported in the perilymph. However, this method was not suitable in humans because the distance between the magnet and the nanoparticle suspension must be less than 2 cm (Du et al., 2013). Thus, a new system of four magnets that pushed nanoparticles into the inner ear was set up allowing larger distances of 3 to 5 cm for the application of the magnets on the treated ear (Sarwar et al., 2013); 300 nm-sized chitosan nanocarriers loaded with SPION and methylprednisolone efficiently protected the inner ear from cisplatin ototoxicity in the long term using this magnetic delivery method (Ramaswamy et al., 2017). In a recent study, another method was used to target the apex of the cochlea (Leterme et al., 2019). The magnet was displaced every 10 minutes to promote SPION displacement all along the turns of cochlea. In 2012, Otomagnetics was created to develop the magnetic delivery for the inner ear, eye and skin (Otomagnetics, 2020). Preclinical studies to evaluate polymer-based nanocarriers loaded with SPION are under way for the protection of the inner ear of children undergoing chemotherapy (Otomagnetics, 2020).

Nevertheless, this strategy needs to verify safety issues due to the long-term residence of inorganic material within the inner ear. In addition, the clinical application must be adjusted according to the position of the round window membrane, which is highly variable in humans (Proctor et al., 1986). Magnetic guidance will require a submillimetric accuracy with coupling to a navigation system to drive the SPION through the magnetic field.

5.3.5. Future strategy: focused ultrasound?

Initially used for diagnosis by echography, ultrasound enhances the permeability of barriers, such as the blood–brain barrier or the skin (Tharkar et al., 2019). Effective nanocarrier delivery to the inner ear has not been demonstrated yet with focused ultrasound, but it has been evaluated for drug delivery (Liao et al., 2020; Shih et al., 2019, 2013). Microbubbles were mixed into a solution of biotin-FITC and injected into the middle ear of guinea pigs (Shih et al., 2013). The ultrasound transducer was applied on the liquid-filled middle ear cavity. After 1 minute of ultrasound exposure, the biotin-FITC concentration in the inner ear was increased by a factor of 3.5. Similarly, a solution of 0.9 mg of dexamethasone phosphate administered by transtympanic injection led to a 10-fold higher concentration in the perilymph using ultrasound (Shih et al., 2019). The combined use of ultrasound and nanocarriers might provide sustained release and an increase in the dexamethasone phosphate concentration in the inner ear. Unlike magnetic delivery, the ultrasound technique might require surgery (Shih et al., 2019). To avoid this, Liao et al. (2020) are currently developing a "transcranial" approach on which the transducer is applied directly to the skull as well as an approach by application of the transducer on the external auditory membrane. These strategies seem closer to a suitable and easy clinical application (Liao et al., 2020), and thus, are promising, particularly for nanocarriers administration. Nevertheless, the safety of focused ultrasound should be assessed.

5.4. Advantages of nanocarriers over drug solutions/hydrogels

The encapsulation of different types of drug (small drugs, siRNA proteins or peptides) within nanocarriers modifies their pharmacokinetic profile by increasing their concentration and/or their residence time in perilymph. This is particularly evidenced for nanocarriers dispersed within hydrogels (Table 3). Nanocarriers also allow the targeting of specific tissues when covered with ligands. For now, the outer hair cells are the only tissue which has been efficiently targeted. Nanocarriers have been proved to migrate into the inner ear, with or without losing their integrity. However, data obtained from longer studies (1 week at least) are needed to quantify the amount of nanocarrier able to cross the barriers to accumulate in the inner ear. Studies evaluating the impact of one unique parameter might allow a better understanding of the key physicochemical parameters governing nanocarrier passage into the inner ear. Clearly, size is key but the surface charge and concentration of the nanocarrier also seem to play an important role.

6. Safety of nanocarrier administration

Before considering the safety of nanocarriers for inner ear delivery, the composition of the formulation must be adapted to the middle and inner ear compartments. It should have a physiological pH (7.38–7.42) and an osmolality around 300 mOsm/kg (El Kechai et al., 2015a). If the pH is controlled, the osmolality is rarely reported although this parameter is crucial. Nanocarriers are often

dispersed in pure water (Cai et al., 2017; Liu et al., 2013a; Meyer et al., 2012), which leads to hypotonic suspensions, or directly incorporated in standard buffers such as phosphate-buffered saline (Lajud et al., 2015; Martín-Saldaña et al., 2018; Roy et al., 2012), which could conversely lead to hypertonic suspensions. Hypotonic or hypertonic suspensions can induce noxious fluid displacements between the perilymph and the suspension *via* the round window (Mikulec et al., 2008). Hearing is extremely sensitive to changes in fluid volume and ionic composition. Thus, a formulation intended for inner ear delivery should respect the homeostasis of inner ear fluids. Furthermore, according to the monography for parenteral preparations in the European Pharmacopeia (Ph. Eur. 10.2, 2020a), the system must be sterile and endotoxin-free.

The safety of a formulation is the evaluation of its effect without any drugs on healthy animals, and the assessment of the function of the targeted organ. For the inner ear, the main outcome to measure is the hearing function, through auditory brainstem response records. The second outcome is the evaluation of the structure of the organ of Corti by histology or an inflammatory response (macrophages, pro-inflammatory cytokines or other markers) which is very important for the evaluation of nanocarrier toxicity on the inner ear. If some nanocarriers cross the inner ear barriers, they might remain in the cochlea for a long time and induce side effects in the long term. Hearing function must be primarily evaluated, because some defects are not visible from histology such as loss of hair cell bundles or conductivity changes (Corey et al., 2017).

A summary of studies carried out on the safety evaluation of different nanocarriers (PEGylated, cationic, anionic, neutral) using passive or advanced strategies is presented below (Table 4). The duration of these studies is very variable: from 1 day up to 3 months but centered around 1 week. The toxicity of nanocarriers on the inner ear was evaluated after intratympanic administration, which is well-tolerated in the clinic, and by intracochlear administration to maximize the nanocarrier concentration in the inner ear (Table 4). The latter technique allows the identification of potential side effects. For example, a dose-dependent toxicity and inflammation were observed after intracochlear injection of cationic liposomes (Staecker et al., 2001) but not after intratympanic administration (Jero et al., 2001b). The toxicity of nanocarriers by intratympanic administration was less pronounced for several reasons: *1)* low passage of nanocarriers into the cochlea, *2)* potential destabilization of nanocarriers in middle ear barriers, *3)* low residence time in the middle ear when they are administered as liquid suspensions. The administration of the nanocarrier is mostly neither repeated nor continuous, although it could be necessary to evaluate the effect of multiple administrations (Table 4). Furthermore, safety studies must be conducted on a broad concentration range of nanocarriers in terms of material or particle concentration that fit clinical practice, because the nanocarrier concentration is adjusted as a function of the drug loading obtained in efficacy studies.

Table 4: Safety of nanocarriers administered by intratympanic or intracochlear routes

Nanocarrier	Nanocarrier characteristics	Study design	Administration	Outcomes regarding safety	Reference
Passive delivery					
Cationic liposomes	ns 0.01 mM	Mouse n = 1/group 1 week	Sponge applied on RWM for 3 days	No histological damage. Slight increase in hearing thresholds.	(Jero et al., 2001a)
Cationic liposomes	ns	Mouse n = 2/group 3 days	Sponge applied on RWM for 3 days or intracochlear injection	No histological damage to the organ of Corti.	(Jero et al., 2001b)
Cationic liposomes	ns 0.005 mM	Guinea pig Number ns 2 weeks	Intracochlear injection or osmotic pump	No inflammation, no lymphocyte or macrophage infiltration. Fibrosis and immunoreactivity at osmotic pump site.	(Wareing et al., 1999)
Cationic liposome	ns	Mouse n = 3/group 3 days	Intracochlear injection	Destruction of organ of Corti in a dose-dependent manner. Inflammation at injection site.	(Staecker et al., 2001)
Cationic PEGylated liposomes	105 ± 15 nm PdI = 0.04 +14 mV 1 mM	Rat n = 14 for the whole study 1 or 20 days	Application on the stapes or on the RWM ± continuously with osmotic pump	No cochlear inflammation and no toxicity up to 20 days.	(Zou et al., 2014b)
Cationic PEGylated liposomes	105 ± 15 nm PdI = 0.04 +14 mV 1 mM	Rat n = 4 for the whole study 1 week	TTI	No histological damage. No glycosaminoglycan expression, no apoptotic cells. Slight increase in hyaluronic acid expression in spiral ligament.	(Zou et al., 2017a)
PEGylated liposomes *versus* **PEGylated polymersomes**	82 nm, PdI = 0.05 1 mM 90 nm 3 mg/mL	Mice n = 30 for the whole study 2 weeks	Sponge applied on RWM for 2 weeks.	No toxicity of nanocarriers on hearing thresholds. No histological damage.	(Buckiová et al., 2012)
Poly(amino acid)-based polymersomes	27 ± 16 nm –35 mV	Mouse n = 4/group 1 day to 1 week	Sponge applied on RWM for 1 day	No impact on hearing thresholds. Swollen middle ear mucosa in nanocarrier group.	(Kim et al., 2015)
PEGylated lipid nanocapsules *versus* **Hyperbranched polylysine**	52 ± 5 nm –55 ± 7 mV 1015 particles/mL 10 nm PdI = 10 0.04 mM	Guinea pig n = 15 for the whole study 1 month	Intracochlear injection	No hair cell loss. No hearing thresholds difference between groups but 10 dB global average loss at day 28.	(Scheper et al., 2009)
PEGylated lipid nanocapsules	52 ± 5 nm 5 ± 1 mV 20.5 mg/mL	Rat Number ns 1 month	Sponge applied on RWM for 3 days	No impact on hearing thresholds at day 7 and day 28. No apoptosis induction. Less innervation of outer hair cells but no impact for inner hair cells.	(Y. Zhang et al., 2011b)
PLGA nanoparticles: - **Uncoated** - **PEGylated** - **Poloxamer-covered** - **Chitosan-covered**	25 mg/mL 158 nm PdI = 0.12 135 nm PdI = 0.17 170 nm PdI = 0.11 155 nm PdI = 0.3	Guinea pig Number ns 1 day	TTI	No inflammation in the inner ear.	(Wen et al., 2016)

ns, not specified; PdI, polydispersity index; PEG, poly(ethylene glycol); PLGA, poly(lactic-co-glycolic acid); RWM, round window membrane; TTI, transtympanic injection.

Table 4: Safety of nanocarriers administered by intratympanic or intracochlear routes (continued)

Nanocarrier	Nanocarrier characteristics	Study design	Administration	Results outcomes regarding safety	Reference
Nanoparticles based on drug-conjugated polymer (tocopherol, tocopheryl succinate, ibuprofen)	128–175 nm	Rat n = 2/group 3 days	TTI	No impact on hearing thresholds.	(Martín-Saldaña et al., 2018, 2017, 2016)
Silver nanoparticles	117 ± 24 nm –20 ± 9 mV 0.02–4 mg/mL	Rat n = 14 for the whole study 1 week	TTI	Barrier permeability changes. Dose-dependent hearing loss, but reversible 5 h post-administration. At 4 mg/mL, 30 dB loss at all frequencies. Cell death in tissues at low doses.	(Zou et al., 2014a)
Streptavidin-covered SPION	200 nm 3.10^{10}–$1.5.10^{12}$ particles/mL	Guinea pig n = 28 for the whole study 1 week	Intracochlear injection	No impact on hearing thresholds.	(Nguyen et al., 2016)
Advanced delivery					
Hyaluronic acid gel containing PEGylated liposomes	146 ± 50 nm PdI = 0.1 –29 mV 80 mM	Guinea pig n = 42 for the whole study 1 month	TTI	No impact on hearing thresholds.	(El Kechai et al., 2016)
A666 peptide-covered gold nanoparticles in hydrogel	52 nm	Mouse Number ns 1 day	TTI	No histological damage induced on hair cells.	(Kayyali et al., 2017)
PLGA nanoparticles ± mixed with protamine: - **Uncoated** - **Poloxamer-coating**	PdI <2 155 ± 5 nm –13 mV 185 ± 10 nm –16 mV	Guinea pig n = 3/group 1 day	TTI	No histological change induced on organ of Corti, spiral ganglion, stria vascularis and RWM after both nanoparticle and low molecular weight protamine administration.	(Cai et al., 2017)
Chitosan nanocarriers containing SPION	300 nm PdI = 0.67 25 mg/mL	Rat n = 12/group 1–3 months	TTI + magnet Single-dose or multi-dose (1/week)	No hearing loss at long-term in single and multi-dose study. Repeated administrations did not increase hearing loss. Slight inflammation in cochlea. No iron particles found in other organs.	(Shimoji et al., 2019)
Chitosan nanocarriers containing SPION	300 nm 25 mg/mL	Rat n = 5/group 1 month	TTI + magnet Single-dose or multi-dose (1/week)	Mild inflammatory changes. Macrophages containing intracytoplasmic iron present in the middle ear. Repeated administrations did not increase inflammation ratio.	(Lafond et al., 2018)
Hyaluronic acid gel containing SPION	135 ± 5 nm 2.5 mg/mL	Rat n = 6 for the whole study 1 month	TTI + magnet	Immediate postoperative shift of hearing thresholds (10–15 dB) at 16 and 32 kHz, reversible at day 7. No impact on hearing thresholds at 2 and 4 kHz.	(Leterme et al., 2019)

ns, not specified; PdI, polydispersity index; PEG, poly(ethylene glycol); PLGA, poly(lactic-co-glycolic acid); RWM, round window membrane; SPION, superparamagnetic iron oxide nanoparticles; TTI, transtympanic injection.

6.1. Safety of the passive administration of nanocarriers

Most of the nanocarriers showed a good safety profile with no impact on hearing function or inner ear structures (Table 4), apart from silver nanoparticles that are ototoxic (Zou et al., 2014a). PEGylated liposomes exhibit a slight increase in hyaluronic acid expression but all other markers of inflammation are not expressed (Zou et al., 2017a). A high toxicity is observed after administration of

cationic liposomes in mice (Staecker et al., 2001), but the cationic lipid (N-[1-(2, 3-dioleyloxy)propyl]-N,N,N-trimethylammonium chloride) used in this study is reported to be quite toxic (Campani et al., 2016).

Despite the number of studies on PLGA nanoparticles, so far their safety has been poorly evaluated in inner ear application (Table 4). Nevertheless, the safety of PLGA microparticles is reported after intracochlear administration in guinea pigs (Ross et al., 2016). A loss of 10 dB is observed at midrange frequencies (8 and 20 kHz) 1 week after administration. According to hair cell count, there is no toxicity induced on the sensory cells. However, PLGA microparticles degrade over time due to hydrolysis of PLGA chains. This might lead to a potentially toxic acidification of the pH within the cochlea (Liu et al., 2006). Consequently, future studies on PLGA nanoparticles should evaluate these parameters.

6.2. Safety of advanced strategies for nanocarrier administration

As these strategies have recently been developed, their safety has not been extensively evaluated. Cell-penetrating peptides and active targeting did not induce obvious histological changes on inner ear structures but have not been evaluated on hearing function (Cai et al., 2017; Kayyali et al., 2018).

On the other hand, the safety of magnetic delivery has been widely evaluated, even at 3 months (Shimoji et al., 2019). Concerns about the accumulation of iron oxide in the inner ear, with potential noxious oxidative properties, are the major limitation for clinical studies. When injected by the intracochlear route, SPION coated with streptavidin do not induce any hearing loss at 1 week (Nguyen et al., 2016). However, that study might be too short for the coating to be degraded and release its content, which may induce toxicity. Otomagnetics shows that chitosan nanocarriers containing SPION do not induce any hearing loss 3 months after administration by magnetic delivery (Shimoji et al., 2019). Slight inflammation is reported. However, another study, also conducted in rats, reports a mild inflammatory response with the same nanocarriers (Lafond et al., 2018). Numerous macrophages infiltrate the round window membrane and the inner ear. SPION are identified inside the cytoplasm of the macrophages. Using a hyaluronic acid gel, SPION organized in clusters of 135 nm are administered by magnetic delivery so that there was only the effect of SPION (Leterme et al., 2019). An immediate but transient hearing loss is observed at high frequencies, thus nearby the round window membrane. However, no other adverse effect has been reported. Thus, it is possible that the adverse reaction observed by Lafond et al. (2018) is due to using chitosan nanocarriers.

7. Therapeutic efficacy of drug-loaded nanocarriers on inner ear disorders

In this section, we give an overview of the therapeutic efficacy of drug-loaded nanocarriers on inner ear disorders. Several drug-loaded nanocarriers with a size between 87 and 300 nm but most

frequently with a mean diameter centered around 150 nm have been tested in preclinical studies. Their characteristics and therapeutic efficacy are summarized in Table 5.

Table 5: Therapeutic efficacy of nanocarriers administered by intratympanic route

Type of nanocarrier	Nanocarrier characteristics	Drug (dose or drug loading %)	Therapeutic application	Study design	Administration	Therapeutic effect	Reference
Passive delivery							
Cationic liposomes	ns	4 different siRNA (0.25–5 µg)	Efficacy to silence GJB2 mutant gene, involved in genetic hearing loss	GJB2- mutant mouse (~20 dB hearing loss) n = 6/group 3 days	Sponge applied on RWM	Liposomes-siRNA decrease mutant GJB2 expression by 70% in the cochlea and do not affect endogenous GJB2. 15 dB of hearing improvement at all frequencies.	(Maeda et al., 2005)
PEGylated PLA nanoparticles	130 nm –26 mV	Dexamethasone (50 µg, 8%)	Efficacy against cisplatin ototoxicity	Guinea pig n = 6/group 3 days	Applied on RWM	Dexamethasone-loaded nanoparticles induce 10 dB of hearing improvement at 4-8 kHz compared to non-encapsulated dexamethasone. No effect at high frequencies. Dexamethasone-loaded nanoparticles protect hair cells (65%) at 6 kHz region compared to dexamethasone phosphate solution (40%).	(Sun et al., 2015)
Methacrylic derivatives of tocopheryl succinate or tocopherol	128 nm –5 mV	Methyl-prednisolone (10 or 15%)	Efficacy against cisplatin ototoxicity	Rat n = 6/group 3 days	TTI	15% methylprednisolone-loaded nanoparticles based on methacrylic derivative of tocopheryl succinate induce 20 dB of hearing improvement at mid-high frequencies. Hair cell protection at cochlea base. No efficacy of 10% methylprednisolone-loaded nanoparticles based on methacrylic derivative of tocopheryl succinate or tocopherol.	(Martín-Saldaña et al., 2016)
Methacrylic derivatives of tocopheryl succinate or tocopherol	~120–140 nm –3 to –7 mV	Tocopheryl succinate (10%) or dexamethasone (15%)	Efficacy against cisplatin ototoxicity	Rat n = 6/group 3 days	TTI	Dexamethasone-loaded nanoparticles based on methacrylic derivative of tocopherol induce 15 dB of hearing improvement at all frequencies. Tocopheryl succinate-loaded nanoparticles based on methacrylic derivative of tocopheryl succinate induce 10 dB of hearing improvement at 12, 20 and 32 kHz. No efficacy of other nanoparticles: dexamethasone-loaded nanoparticles based on methacrylic derivative of tocopheryl succinate, tocopheryl succinate loaded nanoparticles based on methacrylic derivative of tocopherol.	(Martín-Saldaña et al., 2017)
Methacrylic derivatives of tocopheryl succinate, tocopherol or ibuprofen	180–210 nm –5 to 0 mV	Dexamethasone (10%)	Efficacy against cisplatin ototoxicity	Rat n = 3/group 3 days	TTI	Dexamethasone-loaded nanoparticles based on methacrylic derivatives of tocopheryl succinate and ibuprofen induce 10 dB of hearing improvement at all frequencies. No efficacy of dexamethasone-loaded nanoparticles based on methacrylic derivatives of tocopherol and ibuprofen.	(Martín-Saldaña et al., 2018)
Solid lipid nanoparticles	94 nm	Edaravone	Chronic noise exposure to induce hearing loss	Guinea pig n = 96 for the whole study 1 week	TTI	Edaravone-loaded nanoparticles induce 10 dB of hearing improvement compared to untreated and edaravone solution groups. Decrease of free radicals in the inner ear.	(Gao et al., 2015)
Cationic PEGylated lipid nanoemulsions	143 ± 22 nm	Dexamethasone (93 ± 8%, 4.2 µg)	Efficacy against kanamycin ototoxicity	Deafened mouse n = 6/group 1 week	TTI	Dexamethasone-loaded lipid nanocapsules induced 20 dB of hearing improvement compared to dexamethasone suspension group.	(Yang et al., 2018)

ns, not specified; GJB2, gap junction protein beta 2; PEG, poly(ethylene glycol); PLGA, poly(lactic-co-glycolic acid); PLA, polylactic acid; RWM, round window membrane; siRNA, small interfering RNA; TTI, transtympanic injection.

Table 5: Therapeutic efficacy of nanocarriers administered by intratympanic route (continued)

Type of nanocarrier	Nanocarrier characteristics	Drug (dose or drug loading %)	Therapeutic application	Study design	Administration	Therapeutic effect	Reference
Advanced delivery							
Gel containing lipid nanocapsules	ns	N-acetyl-L-cysteine	Efficacy against cisplatin ototoxicity	Guinea pig n = 45 for the whole study 1–3 weeks	TTI	No therapeutic effect on hearing thresholds. Lipid nanocapsules not adapted to encapsulate hydrophilic drugs.	(Mohan et al., 2014)
Hyaluronic acid gel containing PEGylated liposomes	146 ± 50 nm PdI = 0.1 –29 mV	Dexamethasone phosphate (1.5 mg)	Cochlear implantation with manual or robotic insertion	Guinea pig n = 5–8/group 1 week	TTI	Manual insertion + drug-loaded liposomal gel: 10 dB of hearing improvement at all frequencies. Robotic insertion + unloaded liposomal gel: 10 dB of hearing improvement at all frequencies. Robotic insertion + drug-loaded liposomal gel: no additional effect of dexamethasone phosphate.	(Mamelle et al., 2017)
Hyaluronic acid gel containing PEGylated liposomes	146 ± 50 nm PdI = 0.1 –29 mV	Dexamethasone phosphate (1.5 mg)	Noise-induced hearing loss	Guinea pig n = 13/group 1 month	TTI 2 days post trauma	No hearing recovery at 1 week except in control group. Full recovery at 1 month except at 8 kHz.	(Mamelle et al., 2018)
Chitosan-gel containing PEGylated liposomes coated with prestin-targeting peptide-1	87 ± 5 nm	c-Jun kinase inhibitor-1	Permanent noise-induced hearing loss	Mouse n = 10/group 14 days	Applied on RWM 2 days before trauma	Non-targeted drug-loaded PEGylated liposomes induce 20 dB of hearing improvement compared to unloaded PEGylated liposomes. PEGylated liposomes targeting outer hair cells induce 35 dB of hearing improvement on average at all frequencies.	(Kayyali et al., 2018)
PEGylated PLGA nanoparticles coated with A666 peptide	158 ± 14 nm –30 mV	Dexamethasone (0.6 µg)	Efficacy against cisplatin ototoxicity	Guinea pig n = 10/group 3 days	Applied on RWM 1h before cisplatin injection	Peptide-covered dexamethasone-loaded nanoparticles induce, respectively 20 and 10 dB of hearing improvement at low and high frequencies. No efficacy of not-targeted dexamethasone-loaded nanocarriers.	(Wang et al., 2018)
Chitosan nanocarriers containing SPION	300 nm PdI = 0.67	Methyl-prednisolone (0.15 µg)	Efficacy against cisplatin ototoxicity	Mouse n = 6/group 1½ months	TTI + magnet	Drug-loaded nanocarriers with magnetic delivery induce 10 dB of hearing improvement compared to drug solution and increased outer hair cell density compared to drug solution (68 *versus* 50 cells /200 µm).	(Ramaswamy et al., 2017)

ns, not specified; PdI, polydispersity index; PEG, poly(ethylene glycol); PLGA, poly(lactic-co-glycolic acid); RWM, round window membrane; siRNA, small interfering RNA; SPION, superparamagnetic iron oxide nanoparticles; TTI, transtympanic injection.

7.1. Animal models

Animal models used to evaluate the efficacy of nanocarriers pertain exclusively to the cochlea. Indeed, models for diseases impacting the vestibule (Ménière's disease) are difficult to set up (Kapolowicz and Thompson, 2020), and consequently, they have not been evaluated with nanocarriers. Hearing function is measured before and after administration of a treatment. The sensitivity of this measurement is of ±5 dB, thus only a hearing improvement of 10 dB is significant.

The most common animal model used is the protection against cisplatin ototoxicity in rodents. Cisplatin is an anticancer drug widely administered in clinics (Duan et al., 2016) inducing ototoxicity (Paken et al., 2019). The resulting hearing loss is attributed to oxidative stress and inflammation (Gentilin et al., 2019). Other drugs are known to be ototoxic, like aminoglycoside antibiotics (kanamycin, gentamicin) (Xie et al., 2011). Depending on patient inter-variability, these drugs can cause permanent hearing loss in adults and children (Lanvers-Kaminsky and Ciarimboli, 2017). The rodent model is quite easy to set up, but the level of hearing loss depends on the ototoxic drug dose. Thus, studies are not always comparable (Table 5).

Another model is noise-induced hearing loss. The rodent is exposed to a high level of noise over a predetermined time. The hearing loss level is not very reproducible among studies or animals due to several factors such as duration of noise exposure, targeted frequencies, and noise intensity. Moreover, rodents can spontaneously recover hearing with time (Ma et al., 2015).

In the case of the cochlear implant model, the trauma resulting from insertion of the electrode array inside the scala tympani is more reproducible (Mamelle et al., 2017).

The genetic model of hearing loss is quite rare, but gap junction protein β2 gene mutation has recently been developed. It is the most common cause of recessive prelingual genetic deafness (Estivill et al., 1998). In the mutant murine model, the generation of genetic deafness leads to a shift of 20 dB in hearing thresholds (Maeda et al., 2005).

In some studies, nanocarriers are administered before the induction of trauma to maximize the amount of drug directly available in the inner ear. PLGA nanoparticles (Wang et al., 2018) and PEGylated liposomes (Kayyali et al., 2018) are applied 1 hour and 2 days, respectively before trauma. However, one must bear in mind that these conditions must reproduce real life clinical practice. This is not the case for noise-induced hearing loss.

7.2. Efficacy of the drug-loaded nanocarrier over free drug solution

The duration of studies evaluating the efficacy of drug-loaded nanocarriers in suspension is quite short (3 days to 1 week). Indeed, it is adapted to the duration of exposure to the drug after intratympanic administration of nanocarrier suspension (see section 5.1.3).

The benefit of drug-loaded nanocarriers compared to drug solution has been demonstrated for most of the nanocarriers (Table 5). SiRNA-loaded cationic liposomes (Maeda et al., 2005), self-assembled

nanoparticles (Martín-Saldaña et al., 2018, 2017, 2016), dexamethasone-loaded PEGylated nanoemulsions (Yang et al., 2018), dexamethasone-loaded PEGylated PLGA nanoparticles (Sun et al., 2015; Wang et al., 2018) and edaravone-loaded solid lipid nanoparticles (Gao et al., 2015) significantly improve hearing (> 10 dB compared to the control group) in different animal models (Table 5).

Nanocarrier efficacy is generally explained by the rise in drug concentration in the inner ear and the drug residence time (Jero et al., 2001b; Maeda et al., 2005; Sun et al., 2015). However, these factors are not always related. For example, dexamethasone-loaded nanoemulsions are more efficient in protecting against kanamycin ototoxicity compared to the free drug, despite equivalent inner ear drug delivery (Yang et al., 2018).

Among the factors favoring the efficacy of nanocarriers compared to the free drug, the drug loading and final dose administered are very important. A 50 µg dose of encapsulated dexamethasone is more efficient against cisplatin ototoxicity compared to the same dose of free drug (Sun et al., 2015) whereas 0.6 µg of drug (either encapsulated in the nanoparticles or free) is not more efficient in another study with non-targeted PLGA nanoparticles (Wang et al., 2018). For drugs other than corticoids, the dose administered in the control group receiving the free drug is rarely documented (Gao et al., 2015; Kayyali et al., 2018; Mohan et al., 2014).

7.3. Additional efficacy of advanced strategies

We can highlight a trend of recent studies to test the efficacy of hydrogels containing nanocarriers (Table 5). The duration of these studies is longer, more than 1 week compared to those done with nanocarriers alone (see section 5.3). Two hybrid systems combining a hydrogel (chitosan or hyaluronic acid) with drug-loaded PEGylated liposomes protect the cochlea in different models (Kayyali et al., 2018; Mamelle et al., 2017). However, the benefit of hybrid systems over hydrogels has not been assessed because the hydrogel group is not present in animal studies (Kayyali et al., 2018; Mamelle et al., 2017). This is important especially for drugs like D-c-Jun kinase inhibitor-1 which cross the round window membrane easily (Eshraghi et al., 2018). Indeed, the drug release has been shown to be prolonged for hyaluronic acid gel containing PEGylated liposomes (El Kechai et al., 2016). However, most of the reports do not perform drug pharmacokinetic studies (Kayyali et al., 2018; Mohan et al., 2014).

The active targeting of outer hair cells is an efficient strategy (Kayyali et al., 2018; Wang et al., 2018). Drug-loaded targeted nanocarriers provide significant protection against noise or cisplatin ototoxicity. Targeted nanocarriers do not seem to modify the drug release in the perilymph, but they specifically accumulate in the outer hair cells (Wang et al., 2018). For the chitosan gel containing targeted liposomes, the small fraction of targeted liposomes reaching the perilymph (5%) is sufficient to protect the outer hair cells from noise (Kayyali et al., 2018).

Another strategy, the magnetic delivery of methylprednisolone-loaded PLGA nanoparticles (Ramaswamy et al., 2017), has demonstrated its superiority over drug-loaded nanoparticles alone, with a low dose of drug administered compare to other studies (Table 5). This is coherent with the prolonged drug release and the high drug/nanocarrier concentration achieved in pharmacokinetic studies with similar systems (Du et al., 2013; Kopke et al., 2006).

To conclude, all these strategies seem to enhance drug efficacy, by raising the drug concentration in the perilymph and the duration of drug exposure (El Kechai et al., 2016; Ramaswamy et al., 2017). However, the safety of such systems has not always been evaluated (Kayyali et al., 2018; Wang et al., 2018).

8. Conclusion

Nanocarriers for inner ear therapy have undergone rapid progress over this last decade, particularly in combination with advanced strategies. They sustain the drug delivery to the inner ear after intratympanic administration, whether they cross the round window membrane (Kayyali et al., 2018; Ramaswamy et al., 2017) or accumulate in this barrier (El Kechai et al., 2016). The size and surface composition of the nanocarriers are key parameters for their passage across this barrier. When evaluated, the improved efficacy of the nanocarrier is related to the sustained release of the drug (Table 5). This review highlights a clear trend towards the development of nanocarriers incorporated in hydrogels (Dai et al., 2018; Ding et al., 2019; El Kechai et al., 2016; Kayyali et al., 2018), coated with a targeting ligand (Kayyali et al., 2018; Wang et al., 2018), or using a method to increase the permeability of the round window membrane (Cai et al., 2017; Ramaswamy et al., 2017; Yoon et al., 2015). These advanced strategies have proved to be efficient in long-term studies in different animal models and pave the way for the development of new drug delivery systems for the inner ear. Nanocarriers appear to be globally safe for the inner ear. However, the toxicity at long term of some promising systems such as PLGA nanoparticles (Sun et al., 2015; Wen et al., 2016) needs to be evaluated for side effects due to nanocarrier degradation. In the future, cross-sectional studies evaluating nanocarrier biodistribution, drug delivery, safety and efficacy must be developed.

Sample CRediT author statement

Céline JAUDOIN: Conceptualization, Methodology, Investigation, Visualization, Writing - original draft. **Florence AGNELY:** Conceptualization, Supervision, Writing - review & editing, Funding acquisition, Project administration. **Yann NGUYEN:** Writing - review & editing. **Evelyne FERRARY:** Writing - review & editing. **Amélie BOCHOT:** Conceptualization, Supervision, Writing - review & editing, Funding acquisition, Project administration.

Acknowledgements

Céline Jaudoin acknowledges the Ministère de l'Enseignement Supérieur, de la Recherche et de l'Innovation for her PhD grant 2017-110. This work was supported by ANR (The French National Research Agency) (N° ANR-15-CE19-0014-02-04). Yann Nguyen and Evelyne Ferrary acknowledge the "Fondation pour l'Audition" (Hearing Institute starting grant). The authors would like to thank Savina Legrenzi for drawing Figure 1A specifically for this review.

Declaration of interest

The authors declare no conflict of interest.

References

Agrahari, V., Agrahari, V., Mitra, A.K., 2017. Inner ear targeted drug delivery: what does the future hold? Ther. Deliv. 8, 179–184. https://doi.org/10.4155/tde-2017-0001

Albert, C., Huang, N., Tsapis, N., Geiger, S., Rosilio, V., Mekhloufi, G., Chapron, D., Robin, B., Beladjine, M., Nicolas, V., Fattal, E., Agnely, F., 2018. Bare and Sterically Stabilized PLGA Nanoparticles for the Stabilization of Pickering Emulsions. Langmuir 34, 13935–13945. https://doi.org/10.1021/acs.langmuir.8b02558

Alzamil, K.S., Linthicum, F.H., 2000. Extraneous round window membranes and plugs: Possible effect on intratympanic therapy. Ann. Otol. Rhinol. Laryngol. 109, 30–32. https://doi.org/10.1177/000348940010900105

Barriga, H.M.G., Holme, M.N., Stevens, M.M., 2019. Cubosomes: The Next Generation of Smart Lipid Nanoparticles? Angew. Chemie Int. Ed. 58, 2958–2978. https://doi.org/10.1002/anie.201804067

Bento, R.F., Danieli, F., Magalhães, A.T. de M., Gnansia, D., Hoen, M., 2016. Residual Hearing Preservation with the Evo® Cochlear Implant Electrode Array: Preliminary Results. Int. Arch. Otorhinolaryngol. 20, 353–358. https://doi.org/10.1055/s-0036-1572530

Bird, P.A., Begg, E.J., Zhang, M., Keast, A.T., Murray, D.P., Balkany, T.J., 2007. Intratympanic Versus Intravenous Delivery of Methylprednisolone to Cochlear Perilymph. Otol. Neurotol. 28, 1124–1130. https://doi.org/10.1097/mao.0b013e31815aee21

Braun, S., Ye, Q., Radeloff, A., Kiefer, J., Gstoettner, W., Tillein, J., 2011. Protection of inner ear function after cochlear implantation: compound action potential measurements after local application of glucocorticoids in the guinea pig cochlea. ORL. J. Otorhinolaryngol. Relat. Spec. 73, 219–28. https://doi.org/10.1159/000329791

Bu, M., Tang, J., Wei, Y., Sun, Y., Wang, X., Wu, L., Liu, H., 2015. Enhanced bioavailability of nerve growth factor with phytantriol lipid-based crystalline nanoparticles in cochlea. Int. J. Nanomedicine 10, 6879–6889. https://doi.org/10.2147/IJN.S82944

Buckiová, D., Ranjan, S., Newman, T.A., Johnston, A.H., Sood, R., Kinnunen, P.K., Popelář, J., Chumak, T., Syka, J., 2012. Minimally invasive drug delivery to the cochlea through application of nanoparticles to the round window membrane. Nanomedicine 7, 1339–1354. https://doi.org/10.2217/nnm.12.5

Cai, H., Liang, Z., Huang, W., Wen, L., Chen, G., 2017. Engineering PLGA nano-based systems through understanding the influence of nanoparticle properties and cell-penetrating peptides for cochlear drug delivery. Int. J. Pharm. 532, 55–65. https://doi.org/10.1016/j.ijpharm.2017.08.084

Cai, H., Wen, X., Wen, L., Tirelli, N., Zhang, X., Zhang, Y., Su, H., Yang, F., Chen, G., 2014. Enhanced local bioavailability of single or compound drugs delivery to the inner ear through application of plga nanoparticles via round window administration. Int. J. Nanomedicine 9,

5591–5601. https://doi.org/10.2147/ijn.s72555

Campani, V., Salzano, G., Lusa, S., de Rosa, G., 2016. Lipid nanovectors to deliver RNA oligonucleotides in cancer. Nanomaterials 6, 141. https://doi.org/10.3390/nano6070131

Chen, G., Hou, S.X., Hu, P., Jin, M.Z., Liu, J., 2007. Preliminary study on brain-targeted drug delivery via inner ear. Yaoxue Xuebao 42, 1102–1106.

Chidanguro, T., Ghimire, E., Liu, C.H., Simon, Y.C., 2018. Polymersomes: Breaking the Glass Ceiling? Small 14, 1802734. https://doi.org/10.1002/smll.201802734

Cong, V.T., Gaus, K., Tilley, R.D., Gooding, J.J., 2018. Rod-shaped mesoporous silica nanoparticles for nanomedicine: recent progress and perspectives. Expert Opin. Drug Deliv. 15, 881–892. https://doi.org/10.1080/17425247.2018.1517748

Corey, D.P., Ó Maoiléidigh, D., Ashmore, J.F., 2017. Mechanical Transduction Processes in the Hair Cell, in: Manley, G., Gummer, A., Popper, A., Fay, R. (Eds.), Understanding the Cochlea, Springer Handbook of Auditory Research. Springer, Cham, pp. 75–111. https://doi.org/10.1007/978-3-319-52073-5_4

Crommelin, D.J.A., van Hoogevest, P., Storm, G., 2020. The role of liposomes in clinical nanomedicine development. What now? Now what? J. Control. Release 318, 256–263. https://doi.org/10.1016/j.jconrel.2019.12.023

Dai, J., Long, W., Liang, Z., Wen, L., Yang, F., Chen, G., 2018. A novel vehicle for local protein delivery to the inner ear: injectable and biodegradable thermosensitive hydrogel loaded with PLGA nanoparticles. Drug Dev. Ind. Pharm. 44, 89–98. https://doi.org/10.1080/03639045.2017.1373803

Dallos, P., 2008. Cochlear amplification, outer hair cells and prestin. Curr. Opin. Neurobiol. 18, 370–376. https://doi.org/10.1016/j.conb.2008.08.016

De Ceulaer, G., Johnson, S., Yperman, M., Daemers, K., Offeciers, F.E., O'Donoghue, G.M., Govaerts, P.J., 2003. Long-term evaluation of the effect of intracochlear steroid deposition on electrode impedance in cochlear implant patients. Otol. Neurotol. 24, 769–774. https://doi.org/10.1097/00129492-200309000-00014

Degors, I.M.S., Wang, C., Rehman, Z.U., Zuhorn, I.S., 2019. Carriers break barriers in drug delivery: endocytosis and endosomal escape of gene delivery vectors. Acc. Chem. Res. 52, 1750–1760. https://doi.org/10.1021/acs.accounts.9b00177

Demina, T., Grozdova, I., Krylova, O., Zhirnov, A., Istratov, V., Frey, H., Kautz, H., Melik-Nubarov, N., 2005. Relationship between the structure of amphiphilic copolymers and their ability to disturb lipid bilayers. Biochemistry 44, 4042–4054. https://doi.org/10.1021/bi048373q

Ding, S., Xie, S., Chen, W., Wen, L., Wang, J., Yang, F., Chen, G., 2019. Is oval window transport a royal gate for nanoparticle delivery to vestibule in the inner ear? Eur. J. Pharm. Sci. 126, 11–22. https://doi.org/10.1016/j.ejps.2018.02.031

Douchement, D., Terranti, A., Lamblin, J., Salleron, J., Siepmann, F., Siepmann, J., Vincent, C., 2015. Dexamethasone eluting electrodes for cochlear implantation: Effect on residual hearing. Cochlear Implants Int. 16, 195–200. https://doi.org/10.1179/1754762813Y.0000000053

Du, X., Chen, K., Kuriyavar, S., Kopke, R.D., Grady, B.P., Bourne, D.H., Li, W., Dormer, K.J., 2013. Magnetic targeted delivery of dexamethasone acetate across the round window membrane in guinea pigs. Otol. Neurotol. 34, 41–47. https://doi.org/10.1097/MAO.0b013e318277a40e

Duan, X., He, C., Kron, S.J., Lin, W., 2016. Nanoparticle formulations of cisplatin for cancer therapy. Wiley Interdiscip. Rev. Nanomed. Nanobiotechnol. 8, 776–791. https://doi.org/10.1002/wnan.1390

Dumortier, G., Grossiord, J.L., Agnely, F., Chaumeil, J.C., 2006. A Review of Poloxamer 407 Pharmaceutical and Pharmacological Characteristics. Pharm. Res. 23, 2709–2728.

https://doi.org/10.1007/s11095-006-9104-4

El Kechai, N., Agnely, F., Mamelle, E., Nguyen, Y., Ferrary, E., Bochot, A., 2015a. Recent advances in local drug delivery to the inner ear. Int. J. Pharm. 494, 83–101. https://doi.org/10.1016/j.ijpharm.2015.08.015

El Kechai, N., Bochot, A., Huang, N., Nguyen, Y., Ferrary, E., Agnely, F., 2015b. Effect of liposomes on rheological and syringeability properties of hyaluronic acid hydrogels intended for local injection of drugs. Int. J. Pharm. 487, 187–196. https://doi.org/10.1016/j.ijpharm.2015.04.019

El Kechai, N., Geiger, S., Fallacara, A., Cañero Infante, I., Nicolas, V., Ferrary, E., Huang, N., Bochot, A., Agnely, F., 2017. Mixtures of hyaluronic acid and liposomes for drug delivery: Phase behavior, microstructure and mobility of liposomes. Int. J. Pharm. 523, 246–259. https://doi.org/10.1016/j.ijpharm.2017.03.029

El Kechai, N., Mamelle, E., Nguyen, Y., Huang, N., Nicolas, V., Chaminade, P., Yen-Nicolaÿ, S., Gueutin, C., Granger, B., Ferrary, E., Agnely, F., Bochot, A., 2016. Hyaluronic acid liposomal gel sustains delivery of a corticoid to the inner ear. J. Control. Release 226, 248–257. https://doi.org/10.1016/j.jconrel.2016.02.013

Engmér, C., Laurell, G., Bagger-Sjöbäck, D., Rask-Andersen, H., 2008. Immunodefense of the Round Window. Laryngoscope 118, 1057–1062. https://doi.org/10.1097/MLG.0b013e31816b30b0

Enticott, J.C., Eastwood, H.T., Briggs, R.J., Dowell, R.C., O'Leary, S.J., 2011. Methylprednisolone applied directly to the round window reduces dizziness after cochlear implantation: A randomized clinical trial. Audiol. Neurotol. 16, 289–303. https://doi.org/10.1159/000322137

Eshraghi, A.A., Aranke, M., Salvi, R., Ding, D., Coleman, J.K.M., Ocak, E., Mittal, R., Meyer, T., 2018. Preclinical and clinical otoprotective applications of cell-penetrating peptide D-JNKI-1 (AM-111). Hear. Res. 368, 86–91. https://doi.org/10.1016/j.heares.2018.03.003

Estivill, X., Fortina, P., Surrey, S., Rabionet, R., Melchionda, S., D'Agruma, L., Mansfield, E., Rappaport, E., Govea, N., Milà, M., Zelante, L., Gasparini, P., 1998. Connexin-26 mutations in sporadic and inherited sensorineural deafness. Lancet 351, 394–398. https://doi.org/10.1016/S0140-6736(97)11124-2

Gao, G., Liu, Y., Zhou, C.-H., Jiang, P., Sun, J.-J., 2015. Solid lipid nanoparticles loaded with edaravone for inner ear protection after noise exposure. Chin. Med. J. (Engl). 128, 203–9. https://doi.org/10.4103/0366-6999.149202

Ge, X., Jackson, R.L., Liu, J., Harper, E.A., Hoffer, M.E., Wassel, R.A., Dormer, K.J., Kopke, R.D., Balough, B.J., 2007. Distribution of PLGA nanoparticles in chinchilla cochleae. Otolaryngol. Head Neck Surg. 137, 619–623. https://doi.org/10.1016/j.otohns.2007.04.013

Gentilin, E., Simoni, E., Candito, M., Cazzador, D., Astolfi, L., 2019. Cisplatin-Induced Ototoxicity: Updates on Molecular Targets. Trends Mol. Med. 25, 1123–1132. https://doi.org/10.1016/j.molmed.2019.08.002

Ghiz, A.F., Salt, A.N., DeMott, J.E., Henson, M.M., Henson, O.W., Gewalt, S.L., 2001. Quantitative anatomy of the round window and cochlear aqueduct in guinea pigs. Hear. Res. 162, 105–112. https://doi.org/10.1016/S0378-5955(01)00375-6

Gonçalves, M., Mignani, S., Rodrigues, J., Tomás, H., 2020. A glance over doxorubicin based-nanotherapeutics: From proof-of-concept studies to solutions in the market. J. Control. Release 317, 347–374. https://doi.org/10.1016/j.jconrel.2019.11.016

Gopen, Q., Rosowski, J.J., Merchant, S.N., 1997. Anatomy of the normal human cochlear aqueduct with functional implications. Hear. Res. 107, 9–22. https://doi.org/10.1016/S0378-5955(97)00017-8

Goycoolea, M.V., 2001. Clinical aspects of round window membrane permeability under normal and pathological conditions. Acta Otolaryngol. 121, 437–447. https://doi.org/10.1080/000164801300366552

Goycoolea, M.V., Lundman, L., 1997. Round window membrane. Structure function and permeability: A review. Microsc. Res. Tech. 36, 201–211. https://doi.org/10.1002/(SICI)1097-0029(19970201)36:3<201::AID-JEMT8>3.0.CO;2-R

Goycoolea, M.V., Muchow, D., Martinez, G.C., Aguila, P.B., Goycoolea, H.G., Goycoolea, C. V., Schachern, P., Knight, W., 1988a. Permeability of the Human Round-Window Membrane to Cationic Ferritin. Arch. Otolaryngol. Neck Surg. 114, 1247–1251. https://doi.org/10.1001/archotol.1988.01860230041019

Goycoolea, M.V., Muchow, D., Schachern, P., 1988b. Experimental studies on round window structure: Function and permeability. Laryngoscope 98, 1–20. https://doi.org/10.1288/00005537-198806001-00002

Hargunani, C.A., Kempton, J.B., DeGagne, J.M., Trune, D.R., 2006. Intratympanic Injection of Dexamethasone: Time Course of Inner Ear Distribution and Conversion to Its Active Form. Otol. Neurotol. 27, 564–569. https://doi.org/10.1097/01.mao.0000194814.07674.4f

Hayes, S.H., Ding, D., Salvi, R.J., Allman, B.L., 2013. Anatomy and physiology of the external, middle and inner ear, in: Celesia, G. (Ed.), Handbook of Clinical Neurophysiology. Elsevier, pp. 3–23. https://doi.org/10.1016/B978-0-7020-5310-8.00001-6

Hentzer, E., 1969. Ultrastructure of the human tympanic membrane. Acta Otolaryngol. 68, 376–390. https://doi.org/10.3109/00016486909121576

Hirose, K., Hartsock, J.J., Johnson, S., Santi, P., Salt, A.N., 2014. Systemic lipopolysaccharide compromises the blood-labyrinth barrier and increases entry of serum fluorescein into the perilymph. JARO J. Assoc. Res. Otolaryngol. 15, 707–719. https://doi.org/10.1007/s10162-014-0476-6

Inamura, N., Salt, A.N., 1992. Permeability changes of the blood-labyrinth barrier measured in vivo during experimental treatments. Hear. Res. 61, 12–18. https://doi.org/10.1016/0378-5955(92)90030-Q

Jahnke, K., 1975. The fine structure of freeze-fractured intercellular junctions in the Guinea pig inner ear. Acta Otolaryngol. 80, 5–40. https://doi.org/10.3109/00016487509125512

Jero, J., Mhatre, A.N., Tseng, C.J., Stern, R.E., Coling, D.E., Goldstein, J.A., Hong, K., Zheng, W.W., Hoque, A.T.M.S., Lalwani, A.K., 2001a. Cochlear gene delivery through an intact round window membrane in mouse. Hum. Gene Ther. 12, 539–548. https://doi.org/10.1089/104303401300042465

Jero, J., Tseng, C.J., Mhatre, A.N., Lalwani, A.K., 2001b. A surgical approach appropriate for targeted cochlear gene therapy in the mouse. Hear. Res. 151, 106–114. https://doi.org/10.1016/S0378-5955(00)00216-1

Juhn, S.K., Rybak, L.P., Prado, S., 1981. Nature of blood-labyrinth barrier in experimental conditions. Ann. Otol. Rhinol. Laryngol. 90, 135–141. https://doi.org/10.1177/000348948109000208

Kandathil, C.K., Stakhovskaya, O., Leake, P.A., 2016. Effects of brain-derived neurotrophic factor (BDNF) on the cochlear nucleus in cats deafened as neonates. Hear. Res. 342, 134–143. https://doi.org/10.1016/j.heares.2016.10.011

Kapolowicz, M.R., Thompson, L.T., 2020. Plasticity in Limbic Regions at Early Time Points in Experimental Models of Tinnitus. Front. Syst. Neurosci. 13, 88. https://doi.org/10.3389/fnsys.2019.00088

Kashio, A., Sakamoto, T., Kakigi, A., Suzuki, M., Suzukawa, K., Kondo, K., Sato, Y., Asoh, S., Ohta, S., Yamasoba, T., 2012. Topical application of the antiapoptotic TAT-FNK protein prevents aminoglycoside-induced ototoxicity. Gene Ther. 19, 1141–1149. https://doi.org/10.1038/gt.2011.204

Kayyali, M., Brake, L., Ramsey, A., Wright, A., O Malley, B., Daquing Li, D., 2017. A Novel Nano-approach for Targeted Inner Ear Imaging. J. Nanomed. Nanotechnol. 8, 456.

https://doi.org/10.4172/2157-7439.1000456

Kayyali, M.N., Wooltorton, J.R.A., Ramsey, A.J., Lin, M., Chao, T.N., Tsourkas, A., O'Malley, B.W., Li, D., 2018. A novel nanoparticle delivery system for targeted therapy of noise-induced hearing loss. J. Control. Release 279, 243–250. https://doi.org/10.1016/j.jconrel.2018.04.028

Kim, D.K., 2017. Nanomedicine for Inner Ear Diseases: A Review of Recent in Vivo Studies. Biomed Res. Int. 2017, 3098230. https://doi.org/10.1155/2017/3098230

Kim, D.K., Park, S.N., Park, K.H., Park, C.W., Yang, K.J., Kim, J.D., Kim, M.S., 2015. Development of a drug delivery system for the inner ear using poly(amino acid)-based nanoparticles. Drug Deliv. 22, 367–374. https://doi.org/10.3109/10717544.2013.879354

Kim, S.H., Kim, K.X., Raveendran, N.N., Wu, T., Pondugula, S.R., Marcus, D.C., 2009. Regulation of ENaC-mediated sodium transport by glucocorticoids in Reissner's membrane epithelium. Am. J. Physiol. Physiol. 296, C544–C557. https://doi.org/10.1152/ajpcell.00338.2008

Kopke, R.D., Wassel, R.A., Mondalek, F., Grady, B., Chen, K., Liu, J., Gibson, D., Dormer, K.J., 2006. Magnetic Nanoparticles: Inner Ear Targeted Molecule Delivery and Middle Ear Implant. Audiol. Neurotol. 11, 123–133. https://doi.org/10.1159/000090685

Kuthubutheen, J., Smith, L., Hwang, E., Lin, V., 2016. Preoperative steroids for hearing preservation cochlear implantation: A review. Cochlear Implants Int. 17, 63–74. https://doi.org/10.1080/14670100.2016.1148319

Lafond, J.F., Shimoji, M., Ramaswamy, B., Shukoor, M.I., Malik, P., Shapiro, B., Depireux, D.A., 2018. Middle Ear Histopathology Following Magnetic Delivery to the Cochlea of Prednisolone-loaded Iron Oxide Nanoparticles in Rats. Toxicol. Pathol. 46, 101–106. https://doi.org/10.1177/0192623317732028

Lajud, S.A., Nagda, D.A., Qiao, P., Tanaka, N., Civantos, A., Gu, R., Cheng, Z., Tsourkas, A., O'Malley, B.W., Li, D., 2015. A novel chitosan-hydrogel-based nanoparticle delivery system for local inner ear application. Otol. Neurotol. 36, 341–347. https://doi.org/10.1097/MAO.0000000000000445

Lanvers-Kaminsky, C., Ciarimboli, G., 2017. Pharmacogenetics of drug-induced ototoxicity caused by aminoglycosides and cisplatin. Pharmacogenomics 18, 1683–1695. https://doi.org/10.2217/pgs-2017-0125

Laurell, G.F.E., Teixeira, M., Duan, M., Sterkers, O., Ferrary, E., 2008. Intact blood-perilymph barrier in the rat after impulse noise trauma. Acta Otolaryngol. 128, 608–612. https://doi.org/10.1080/00016480701644102

Le, T.N., Blakley, B.W., 2017. Mannitol and the blood-labyrinth barrier. J. Otolaryngol. Head Neck Surg. 46, 66. https://doi.org/10.1186/s40463-017-0245-8

Lechner, M., Sutton, L., Ferguson, M., Abbas, Y., Sandhu, J., Shaida, A., 2019. Intratympanic Steroid Use for Sudden Sensorineural Hearing Loss: Current Otolaryngology Practice. Ann. Otol. Rhinol. Laryngol. 128, 490–502. https://doi.org/10.1177/0003489419828759

Leterme, G., Guigou, C., Oudot, A., Collin, B., Boudon, J., Millot, N., Geissler, A., Belharet, K., Bozorg Grayeli, A., 2019. Superparamagnetic Nanoparticle Delivery to the Cochlea Through Round Window by External Magnetic Field: Feasibility and Toxicity. Surg. Innov. 26, 646–655. https://doi.org/10.1177/1553350619867217

Li, L., Chao, T., Brant, J., O'Malley, B., Tsourkas, A., Li, D., 2017. Advances in nano-based inner ear delivery systems for the treatment of sensorineural hearing loss. Adv. Drug Deliv. Rev. 108, 2–12. https://doi.org/10.1016/j.addr.2016.01.004

Liao, A.-H., Wang, C.-H., Weng, P.-Y., Lin, Y.-C., Wang, H., Chen, H.-K., Liu, H.-L., Chuang, H.-C., Shih, C.-P., 2020. Ultrasound-induced microbubble cavitation via a transcanal or transcranial approach facilitates inner ear drug delivery. JCI Insight. https://doi.org/10.1172/jci.insight.132880

Liu, H., Chen, S., Zhou, Y., Che, X., Bao, Z., Li, S., Xu, J., 2013a. The effect of surface charge of glycerol monooleate-based nanoparticles on the round window membrane permeability and cochlear distribution. J. Drug Target. 21, 846–854. https://doi.org/10.3109/1061186X.2013.829075

Liu, H., Ding, D.L., Jiang, H.Y., Wu, X.W., Salvi, R., Sun, H., 2011. Ototoxic destruction by co-administration of kanamycin and ethacrynic acid in rats. J. Zhejiang Univ. Sci. B 12, 853–861. https://doi.org/10.1631/jzus.B1100040

Liu, H., Slamovich, E.B., Webster, T.J., 2006. Less harmful acidic degradation of poly(lactic-co-glycolic acid) bone tissue engineering scaffolds through titania nanoparticle addition. Int. J. Nanomedicine 1, 541–545. https://doi.org/10.2147/nano.2006.1.4.541

Liu, H., Wang, Y., Wang, Q., Li, Z., Zhou, Y., Zhang, Y., Li, S., 2013b. Protein-bearing cubosomes prepared by liquid precursor dilution: Inner ear delivery and pharmacokinetic study following intratympanic administration. J. Biomed. Nanotechnol. 9, 1784–1793. https://doi.org/10.1166/jbn.2013.1685

Liu, Y.-C., Chi, F.-H., Yang, T.-H., Liu, T.-C., 2016. Assessment of complications due to intratympanic injections. World J. Otorhinolaryngol. Neck Surg. 2, 13–16. https://doi.org/10.1016/j.wjorl.2015.11.001

Lysaght, A.C., Kao, S.Y., Paulo, J.A., Merchant, S.N., Steen, H., Stankovic, K.M., 2011. Proteome of human perilymph. J. Proteome Res. 10, 3845–3851. https://doi.org/10.1021/pr200346q

Ma, L., Yi, H.J., Yuan, F.Q., Guo, W.W., Yang, S.M., 2015. An efficient strategy for establishing a model of sensorineural deafness in rats. Neural Regen. Res. 10, 1683–1689. https://doi.org/10.4103/1673-5374.153704

Mäder, K., Lehner, E., Liebau, A., Plontke, S., 2018. Controlled drug release to the inner ear: Concepts, materials, mechanisms, and performance. Hear. Res. 368, 49–66. https://doi.org/10.1016/j.heares.2018.03.006

Maeda, Y., Fukushima, K., Nishizaki, K., Smith, R.J.H., 2005. In vitro and in vivo suppression of GJB2 expression by RNA interference. Hum. Mol. Genet. 14, 1641–1650. https://doi.org/10.1093/hmg/ddi172

Mamelle, E., El Kechai, N., Adenis, V., Nguyen, Y., Sterkers, O., Agnely, F., Bochot, A., Edeline, J.M., Ferrary, E., 2018. Assessment of the efficacy of a local steroid rescue treatment administered 2 days after a moderate noise-induced trauma in guinea pig. Acta Otolaryngol. 138, 610–616. https://doi.org/10.1080/00016489.2018.1438659

Mamelle, E., El Kechai, N., Granger, B., Sterkers, O., Bochot, A., Agnely, F., Ferrary, E., Nguyen, Y., 2017. Effect of a liposomal hyaluronic acid gel loaded with dexamethasone in a guinea pig model after manual or motorized cochlear implantation. Eur. Arch. Otorhinolaryngol. 274, 729–736. https://doi.org/10.1007/s00405-016-4331-8

Marshak, T., Steiner, M., Kaminer, M., Levy, L., Shupak, A., 2014. Prevention of cisplatin-induced hearing loss by intratympanic dexamethasone: A randomized controlled study. Otolaryngol. Head Neck Surg. (United States) 150, 983–990. https://doi.org/10.1177/0194599814524894

Martín-Saldaña, S., Palao-Suay, R., Aguilar, M.R., García-Fernández, L., Arévalo, H., Trinidad, A., Ramírez-Camacho, R., San Román, J., 2018. pH-sensitive polymeric nanoparticles with antioxidant and anti-inflammatory properties against cisplatin-induced hearing loss. J. Control. Release 270, 53–64. https://doi.org/10.1016/j.jconrel.2017.11.032

Martín-Saldaña, S., Palao-Suay, R., Aguilar, M.R., Ramírez-Camacho, R., San Román, J., 2017. Polymeric nanoparticles loaded with dexamethasone or α-tocopheryl succinate to prevent cisplatin-induced ototoxicity. Acta Biomater. 53, 199–210. https://doi.org/10.1016/j.actbio.2017.02.019

Martín-Saldaña, S., Palao-Suay, R., Trinidad, A., Aguilar, M.R., Ramírez-Camacho, R., San Román,

J., 2016. Otoprotective properties of 6α-methylprednisolone-loaded nanoparticles against cisplatin: In vitro and in vivo correlation. Nanomed. Nanotechnol. Biol. Med. 12, 965–976. https://doi.org/10.1016/J.NANO.2015.12.367

Maynard, R.L., Downes, N., 2019. The Ear, in: Anatomy and Histology of the Laboratory Rat in Toxicology and Biomedical Research. Elsevier, pp. 293–302. https://doi.org/10.1016/B978-0-12-811837-5.00023-X

Mazzoni, A., 1990. The vascular anatomy of the vestibular labyrinth in man. Acta Otolaryngol. 110, 1–83. https://doi.org/10.3109/00016489009121137

Meyer, H., Stöver, T., Fouchet, F., Bastiat, G., Saulnier, P., Bäumer, W., Lenarz, T., Scheper, V., 2012. Lipidic nanocapsule drug delivery: neuronal protection for cochlear implant optimization. Int. J. Nanomedicine 7, 2449–64. https://doi.org/10.2147/IJN.S29712

Mikulec, A.A., Hartsock, J.J., Salt, A.N., 2008. Permeability of the round window membrane is influenced by the composition of applied drug solutions and by common surgical procedures. Otol. Neurotol. 29, 1020–1026. https://doi.org/10.1097/MAO.0b013e31818658ea

Mikulec, A.A., Plontke, S.K., Hartsock, J.J., Salt, A.N., 2009. Entry of substances into perilymph through the bone of the otic capsule after intratympanic applications in guinea pigs: implications for local drug delivery in humans. Otol. Neurotol. 30, 131–138.

Mittal, R., Pena, S.A., Zhu, A., Eshraghi, N., Fesharaki, A., Horesh, E.J., Mittal, J., Eshraghi, A.A., 2019. Nanoparticle-based drug delivery in the inner ear: current challenges, limitations and opportunities. Artif. Cell. Nanomed. Biotechnol. 47, 1312–1320. https://doi.org/10.1080/21691401.2019.1573182

Mohammadi, A., Jufas, N., Sale, P., Lee, K., Patel, N., O'Leary, S., 2017. Micro-CT analysis of the anatomical characteristics of the stapedial annular ligament. Anat. Sci. Int. 92, 262–266. https://doi.org/10.1007/s12565-016-0331-4

Mohan, S., Smyth, B.J., Namin, A., Phillips, G., Gratton, M.A., 2014. Targeted Amelioration of Cisplatin-Induced Ototoxicity in Guinea Pigs. Otolaryngol. Neck Surg. 151, 836–839. https://doi.org/10.1177/0194599814544877

Nguyen, Y., Celerier, C., Pszczolinski, R., Claver, J., Blank, U., Ferrary, E., Sterkers, O., 2016. Superparamagnetic nanoparticles as vectors for inner ear treatments: Driving and toxicity evaluation. Acta Otolaryngol. 136, 402–408. https://doi.org/10.3109/00016489.2015.1129069

Nicolas, J., Vauthier, C., 2011. Poly(Alkyl Cyanoacrylate) Nanosystems, in: Intracellular Delivery, Fundamental Biomedical Technologies. Springer, Dordrecht, pp. 225–250. https://doi.org/10.1007/978-94-007-1248-5_9

Nomura, Y., 1984. Otological significance of the round window. Adv. Otorhinolaryngol. 33, 1–162. https://doi.org/10.1177/000348948409300625

Nyberg, S., Joan Abbott, N., Shi, X., Steyger, P.S., Dabdoub, A., 2019. Delivery of therapeutics to the inner ear: The challenge of the blood-labyrinth barrier. Sci. Transl. Med. 11, eaao0935. https://doi.org/10.1126/scitranslmed.aao0935

Ohashi, M., Ide, S., Kimitsuki, T., Komune, S., Suganuma, T., 2006. Three-dimensional regular arrangement of the annular ligament of the rat stapediovestibular joint. Hear. Res. 213, 11–16. https://doi.org/10.1016/j.heares.2005.11.007

Ohashi, M., Ide, S., Sawaguchi, A., Suganuma, T., Kimitsuki, T., Komune, S., 2008. Histochemical localization of the extracellular matrix components in the annular ligament of rat stapediovestibular joint with special reference to fibrillin, 36-kDa microfibril-associated glycoprotein (MAGP-36), and hyaluronic acid. Med. Mol. Morphol. 41, 28–33. https://doi.org/10.1007/s00795-007-0394-3

Ohyama, K., Salt, A.N., Thalmann, R., 1988. Volume flow rate of perilymph in the guinea-pig cochlea. Hear. Res. 35, 119–129. https://doi.org/10.1016/0378-5955(88)90111-6

Okuno, H., Sando, I., 1988. Anatomy of the round window: A histopathological study with a graphic reconstruction method. Acta Otolaryngol. 106, 55–63. https://doi.org/10.3109/00016488809107371

Otomagnetics, 2020. Technology | Otomagnetics, Inc. [WWW Document]. URL https://otomagnetics.net/technology (accessed 1.20.20).

Otonomy, Inc. [WWW Document], 2020. URL https://www.otonomy.com/about/ (accessed 3.17.20).

Paasche, G., Bockel, F., Tasche, C., Lesinski-Schiedat, A., Lenarz, T., 2006. Changes of postoperative impedances in cochlear implant patients: The short-term effects of modified electrode surfaces and intracochlear corticosteroids. Otol. Neurotol. 27, 639–647. https://doi.org/10.1097/01.mao.0000227662.88840.61

Paciello, F., Fetoni, A.R., Rolesi, R., Wright, M.B., Grassi, C., Troiani, D., Paludetti, G., 2018. Pioglitazone represents an effective therapeutic target in preventing oxidative/inflammatory cochlear damage induced by noise exposure. Front. Pharmacol. 9, 1103. https://doi.org/10.3389/fphar.2018.01103

Paken, J., Govender, C.D., Pillay, M., Sewram, V., 2019. A Review of Cisplatin-Associated Ototoxicity. Semin. Hear. 40, 108–121. https://doi.org/10.1055/s-0039-1684041

Palao-Suay, R., Aguilar, M.R., Parra-Ruiz, F.J., Fernández-Gutiérrez, M., Parra, J., Sánchez-Rodríguez, C., Sanz-Fernández, R., Rodrigáñez, L., Román, J.S., 2015. Anticancer and antiangiogenic activity of surfactant-free nanoparticles based on self-assembled polymeric derivatives of vitamin E: Structure-activity relationship. Biomacromolecules 16, 1566–1581. https://doi.org/10.1021/acs.biomac.5b00130

Park, I.K., Lasiene, J., Chou, S.H., Horner, P.J., Pun, S.H., 2007. Neuron-specific delivery of nucleic acids mediated by Tet1-modified poly(ethylenimine). J. Gene Med. 9, 691–702. https://doi.org/10.1002/jgm.1062

Patel, M., 2017. Intratympanic corticosteroids in Ménière's disease: A mini-review. J. Otol. 12, 117–124. https://doi.org/10.1016/j.joto.2017.06.002

Ph. Eur. 10.2, 2020a. Parenteral preparations 0520E.

Ph. Eur. 10.2, 2020b. Ear preparations 0652E.

Plontke, S.K., Mikulec, A.A., Salt, A.N., 2008. Rapid clearance of methylprednisolone after intratympanic application in humans. comment on: Bird,P.A., Begg, E.J., Zhang, M., et al. intratympanic versus intravenous delivery of methylprednisolone to cochlear perilymph. otol neurotol 2007;28:1124–1130. Otol. Neurotol. 29, 732–733. https://doi.org/10.1097/MAO.0b013e318173fcea

Plontke, S.K., Salt, A.N., 2018. Local drug delivery to the inner ear: Principles, practice, and future challenges. Hear. Res. 368, 1–2. https://doi.org/10.1016/j.heares.2018.06.018

Pritz, C.O., Dudás, J., Rask-Andersen, H., Schrott-Fischer, A., Glueckert, R., 2013. Nanomedicine strategies for drug delivery to the ear. Nanomedicine 8, 1155–1172. https://doi.org/10.2217/nnm.13.104

Proctor, B., Bollobas, B., Niparko, J.K., 1986. Anatomy of the round window niche. Ann. Otol. Rhinol. Laryngol. 95, 444–446. https://doi.org/10.1177/000348948609500502

Pyykkö, I., Zou, J., Schrott-Fischer, A., Glueckert, R., Kinnunen, P., 2016. An overview of nanoparticle based delivery for treatment of inner ear disorders. Methods Mol. Biol. 1427, 363–415. https://doi.org/10.1007/978-1-4939-3615-1_21

Qi, W., Ding, D., Zhu, H., Lu, D., Wang, Y., Ding, J., Yan, W., Jia, M., Guo, Y., 2014. Efficient siRNA transfection to the inner ear through the intact round window by a novel proteidic delivery technology in the chinchilla. Gene Ther. 21, 10–18. https://doi.org/10.1038/gt.2013.49

Qu, Y., Tang, J., Liu, L., Song, L.L., Chen, S., Gao, Y., 2019. α-Tocopherol liposome loaded chitosan

hydrogel to suppress oxidative stress injury in cardiomyocytes. Int. J. Biol. Macromol. 125, 1192–1202. https://doi.org/10.1016/j.ijbiomac.2018.09.092

Ramaswamy, B., Roy, S., Apolo, A.B., Shapiro, B., Depireux, D.A., 2017. Magnetic Nanoparticle Mediated Steroid Delivery Mitigates Cisplatin Induced Hearing Loss. Front. Cell. Neurosci. 11, 268. https://doi.org/10.3389/fncel.2017.00268

Ramekers, D., Versnel, H., Strahl, S.B., Klis, S.F.L., Grolman, W., 2015. Temporary Neurotrophin Treatment Prevents Deafness-Induced Auditory Nerve Degeneration and Preserves Function. J. Neurosci. 35, 12331–12345. https://doi.org/10.1523/JNEUROSCI.0096-15.2015

Rask-Andersen, H., Schrott-Fischer, A., Pfaller, K., Glueckert, R., 2006. Perilymph/modiolar communication routes in the human cochlea. Ear Hear. 27, 457–465. https://doi.org/10.1097/01.aud.0000233864.32183.81

Richardson, R.T., Wise, A.K., Thompson, B.C., Flynn, B.O., Atkinson, P.J., Fretwell, N.J., Fallon, J.B., Wallace, G.G., Shepherd, R.K., Clark, G.M., O'Leary, S.J., 2009. Polypyrrole-coated electrodes for the delivery of charge and neurotrophins to cochlear neurons. Biomaterials 30, 2614–2624. https://doi.org/10.1016/j.biomaterials.2009.01.015

Roche, J.P., Hansen, M.R., 2015. On the Horizon: Cochlear Implant Technology. Otolaryngol. Clin. North Am. 48, 1097–1116. https://doi.org/10.1016/j.otc.2015.07.009

Ross, A.M., Rahmani, S., Prieskorn, D.M., Dishman, A.F., Miller, J.M., Lahann, J., Altschuler, R.A., 2016. Persistence, distribution, and impact of distinctly segmented microparticles on cochlear health following in vivo infusion. J. Biomed. Mater. Res. Part A 104, 1510–1522. https://doi.org/10.1002/jbm.a.35675

Roy, S., Glueckert, R., Johnston, A.H., Perrier, T., Bitsche, M., Newman, T.A., Saulnier, P., Schrott-Fischer, A., 2012. Strategies for drug delivery to the human inner ear by multifunctional nanoparticles. Nanomedicine 7, 55–63. https://doi.org/10.2217/nnm.11.84

Sakamoto, T., Hiraumi, H., 2014. Anatomy of the inner ear, in: Ito, J. (Ed.), Regenerative Medicine for the Inner Ear. Springer, Japan, pp. 3–13. https://doi.org/10.1007/978-4-431-54862-1_1

Salt, A.N., Gill, R.M., Hartsock, J.J., 2015. Perilymph Kinetics of FITC-Dextran Reveals Homeostasis Dominated by the Cochlear Aqueduct and Cerebrospinal Fluid. JARO J. Assoc. Res. Otolaryngol. 16, 357–371. https://doi.org/10.1007/s10162-015-0512-1

Salt, A.N., Hartsock, J.J., Gill, R.M., King, E., Kraus, F.B., Plontke, S.K., 2016. Perilymph pharmacokinetics of locally-applied gentamicin in the guinea pig. Hear. Res. 342, 101–111. https://doi.org/10.1016/j.heares.2016.10.003

Salt, A.N., Hirose, K., 2018. Communication pathways to and from the inner ear and their contributions to drug delivery. Hear. Res. 362, 25–37. https://doi.org/10.1016/j.heares.2017.12.010

Salt, A.N., King, E.B., Hartsock, J.J., Gill, R.M., O'Leary, S.J., 2012. Marker entry into vestibular perilymph via the stapes following applications to the round window niche of guinea pigs. Hear. Res. 283, 14–23. https://doi.org/10.1016/j.heares.2011.11.012

Salt, A.N., Plontke, S.K., 2018. Pharmacokinetic principles in the inner ear: Influence of drug properties on intratympanic applications. Hear. Res. 368, 28–40. https://doi.org/10.1016/j.heares.2018.03.002

Salt, A.N., Plontke, S.K., 2009. Principles of local drug delivery to the inner ear. Audiol. Neurotol. 14, 350–360. https://doi.org/10.1159/000241892

Salt, A.N., Stopp, P.E., 1979. The effect of cerebrospinal fluid pressure on perilymphatic flow in the opened cochlea. Acta Otolaryngol. 88, 198–202. https://doi.org/10.3109/00016487909137160

Santa Maria, P.L., Domville-Lewis, C., Sucher, C.M., Chester-Browne, R., Atlas, M.D., 2013. Hearing Preservation Surgery for Cochlear Implantation—Hearing and Quality of Life After 2

Years. Otol. Neurotol. 34, 526–531. https://doi.org/10.1097/MAO.0b013e318281e0c9

Santi, P.A., Mancini, P., Barnes, C., 1994. Identification and localization of the GM1 ganglioside in the cochlea using thin-layer chromatography and cholera toxin. J. Histochem. Cytochem. 42, 705–716. https://doi.org/10.1177/42.6.8189033

Sarwar, A., Lee, R., Depireux, D.A., Shapiro, B., 2013. Magnetic injection of nanoparticles into rat inner ears at a human head working distance. IEEE Trans. Magn. 49, 440–452. https://doi.org/10.1109/TMAG.2012.2221456

Scheibe, F., Haupt, H., 1985. Biochemical differences between perilymph, cerebrospinal fluid and blood plasma in the guinea pig. Hear. Res. 17, 61–66. https://doi.org/10.1016/0378-5955(85)90131-5

Scheper, V., Wolf, M., Scholl, M., Kadlecova, Z., Perrier, T., Klok, H.A., Saulnier, P., Lenarz, T., Stöver, T., 2009. Potential novel drug carriers for inner ear treatment: Hyperbranched polylysine and lipid nanocapsules. Nanomedicine 4, 623–635. https://doi.org/10.2217/nnm.09.41

Schilder, A.G.M., Su, M.P., Blackshaw, H., Lustig, L., Staecker, H., Lenarz, T., Safieddine, S., Gomes-Santos, C.S., Holme, R., Warnecke, A., 2019. Hearing Protection, Restoration, and Regeneration: An Overview of Emerging Therapeutics for Inner Ear and Central Hearing Disorders. Otol. Neurotol. 40, 559–570. https://doi.org/10.1097/MAO.0000000000002194

Shepherd, R.K., Coco, A., Epp, S.B., 2008. Neurotrophins and electrical stimulation for protection and repair of spiral ganglion neurons following sensorineural hearing loss. Hear. Res. 242, 100–109. https://doi.org/10.1016/j.heares.2007.12.005

Shi, X., 2016. Pathophysiology of the cochlear intrastrial fluid-blood barrier (review). Hear. Res. 338, 52–63. https://doi.org/10.1016/j.heares.2016.01.010

Shih, C.P., Chen, H.C., Chen, H.K., Chiang, M.C., Sytwu, H.K., Lin, Y.C., Li, S.L., Shih, Y.F., Liao, A.H., Wang, C.H., 2013. Ultrasound-aided microbubbles facilitate the delivery of drugs to the inner ear via the round window membrane. J. Control. Release 167, 167–174. https://doi.org/10.1016/j.jconrel.2013.01.028

Shih, C.P., Chen, H.C., Lin, Y.C., Chen, H.K., Wang, H., Kuo, C.Y., Lin, Y.Y., Wang, C.H., 2019. Middle-ear dexamethasone delivery via ultrasound microbubbles attenuates noise-induced hearing loss. Laryngoscope 129, 1907–1914. https://doi.org/10.1002/lary.27713

Shimoji, M., Ramaswamy, B., Shukoor, M.I., Benhal, P., Broda, A., Kulkarni, S., Malik, P., McCaffrey, B., Lafond, J.F., Nacev, A., Weinberg, I.N., Shapiro, B., Depireux, D.A., 2019. Toxicology study for magnetic injection of prednisolone into the rat cochlea. Eur. J. Pharm. Sci. 126, 33–48. https://doi.org/10.1016/j.ejps.2018.06.011

Silva, S., Almeida, A.J., Vale, N., 2019. Combination of cell-penetrating peptides with nanoparticles for therapeutic application: A review. Biomolecules 9, E22. https://doi.org/10.3390/biom9010022

Silverstein, H., Thompson, J., Rosenberg, S.I., Brown, N., Light, J., 2004. Silverstein MicroWick. Otolaryngol. Clin. North Am. 37, 1019–1034. https://doi.org/10.1016/j.otc.2004.04.002

Smouha, E., 2013. Inner ear disorders. NeuroRehabilitation 32, 455–462. https://doi.org/10.3233/NRE-130868

Staecker, H., Li, D., O'Malley, B.W., Van De Water, T.R., 2001. Gene expression in the mammalian cochlea: A study of multiple vector systems. Acta Otolaryngol. 121, 157–163. https://doi.org/10.1080/000164801300043307

Staecker, H., Rodgers, B., 2013. Developments in delivery of medications for inner ear disease. Expert Opin. Drug Deliv. 10, 639–650. https://doi.org/10.1517/17425247.2013.766167

Suckfuell, M., Lisowska, G., Domka, W., Kabacinska, A., Morawski, K., Bodlaj, R., Klimak, P., Kostrica, R., Meyer, T., 2014. Efficacy and safety of AM-111 in the treatment of acute

sensorineural hearing loss: A double-blind, randomized, placebo-controlled phase II study. Otol. Neurotol. 35, 1317–1326. https://doi.org/10.1097/MAO.0000000000000466

Sun, C., Wang, Xueling, Zheng, Z., Chen, D., Wang, Xiaoqin, Shi, F., Yu, D., Wu, H., 2015. A single dose of dexamethasone encapsulated in polyethylene glycol-coated polylactic acid nanoparticles attenuates cisplatin-induced hearing loss following round window membrane administration. Int. J. Nanomedicine 10, 3567–3579. https://doi.org/10.2147/IJN.S77912

Surovtseva, E.V., Johnston, A.H., Zhang, W., Zhang, Y., Kim, A., Murakoshi, M., Wada, H., Newman, T.A., Zou, J., Pyykkö, I., 2012. Prestin binding peptides as ligands for targeted polymersome mediated drug delivery to outer hair cells in the inner ear. Int. J. Pharm. 424, 121–127. https://doi.org/10.1016/j.ijpharm.2011.12.042

Suzuki, M., Yamasoba, T., Ishibashi, T., Miller, J.M., Kaga, K., 2002. Effect of noise exposure on blood-labyrinth barrier in guinea pigs. Hear. Res. 164, 12–18. https://doi.org/10.1016/S0378-5955(01)00397-5

Swan, E.E.L., Peppi, M., Chen, Z., Green, K.M., Evans, J.E., McKenna, M.J., Mescher, M.J., Kujawa, S.G., Sewell, W.F., 2009. Proteomics analysis of perilymph and cerebrospinal fluid in mouse. Laryngoscope 119, 953–958. https://doi.org/10.1002/lary.20209

Takeda, H., Kurioka, T., Kaitsuka, T., Tomizawa, K., Matsunobu, T., Hakim, F., Mizutari, K., Miwa, T., Yamada, T., Ise, M., Shiotani, A., Yumoto, E., Minoda, R., 2016. Protein transduction therapy into cochleae via the round window niche in guinea pigs. Mol. Ther. Methods Clin. Dev. 3, 16055. https://doi.org/10.1038/mtm.2016.55

Tamura, T., Kita, T., Nakagawa, T., Endo, T., Kim, T.S., Ishihara, T., Mizushima, Y., Higaki, M., Ito, J., 2005. Drug delivery to the cochlea using PLGA nanoparticles. Laryngoscope 115, 2000–2005. https://doi.org/10.1097/01.mlg.0000180174.81036.5a

Tharkar, P., Varanasi, R., Wong, W.S.F., Jin, C.T., Chrzanowski, W., 2019. Nano-Enhanced Drug Delivery and Therapeutic Ultrasound for Cancer Treatment and Beyond. Front. Bioeng. Biotechnol. 7, 324. https://doi.org/10.3389/fbioe.2019.00324

Uchegbu, I.F., Siew, A., 2013. Nanomedicines and nanodiagnostics come of age. J. Pharm. Sci. 102, 305–310. https://doi.org/10.1002/jps.23377

Van De Heyning, P., Muehlmeier, G., Cox, T., Lisowska, G., Maier, H., Morawski, K., Meyer, T., 2014. Efficacy and safety of AM-101 in the treatment of acute inner ear tinnitus - A double-blind, randomized, placebo-controlled phase II study. Otol. Neurotol. 35, 589–597. https://doi.org/10.1097/MAO.0000000000000268

Vigani, B., Rossi, S., Sandri, G., Bonferoni, M.C., Caramella, C.M., Ferrari, F., 2019. Hyaluronic acid and chitosan-based nanosystems: a new dressing generation for wound care. Expert Opin. Drug Deliv. 16, 715–740. https://doi.org/10.1080/17425247.2019.1634051

Wang, X., Chen, Y., Tao, Y., Gao, Y., Yu, D., Wu, H., 2018. A666-conjugated nanoparticles target prestin of outer hair cells preventing cisplatin-induced hearing loss. Int. J. Nanomedicine 13, 7517–7531. https://doi.org/10.2147/IJN.S170130

Wang, X., Dellamary, L., Fernandez, R., Ye, Q., Lebel, C., Piu, F., 2011. Principles of inner ear sustained release following intratympanic administration. Laryngoscope 121, 385–391. https://doi.org/10.1002/lary.21370

Wangemann, P., Marcus, D.C., 2017. Ion and Fluid Homeostasis in the Cochlea, in: Manley, G., Gummer, A., Popper, A., Fay, R. (Eds.), Understanding the Cochlea, Springer Handbook of Auditory Research. Springer, Cham, pp. 253–286. https://doi.org/10.1007/978-3-319-52073-5_9

Wareing, M., Mhatre, A.N., Pettis, R., Han, J.J., Haut, T., Pfister, M.H., Hong, K., Zheng, W.W., Lalwani, A.K., 1999. Cationic liposome mediated transgene expression in the guinea pig cochlea. Hear. Res. 128, 61–69. https://doi.org/10.1016/s0378-5955(98)00196-8

Weckel, A., Marx, M., Esteve-Fraysse, M.J., 2018. Control of vertigo in Ménière's disease by

intratympanic dexamethasone. Eur. Ann. Otorhinolaryngol. Head Neck Dis. 135, 7–10. https://doi.org/10.1016/j.anorl.2017.07.002

Wen, X., Ding, S., Cai, H., Wang, J., Wen, L., Yang, F., Chen, G., 2016. Nanomedicine strategy for optimizing delivery to outer hair cells by surface-modified poly(lactic/glycolic acid) nanoparticles with hydrophilic molecules. Int. J. Nanomedicine 11, 5959–5969. https://doi.org/10.2147/IJN.S116867

World Health Organization, 2019. Deafness and hearing loss [WWW Document]. URL https://www.who.int/news-room/fact-sheets/detail/deafness-and-hearing-loss (accessed 1.14.20).

Wu, N., Li, M., Chen, Z.T., Zhang, X.B., Liu, H.Z., Li, Z., Guo, W.W., Zhao, L.D., Ren, L.L., Li, J.N., Yi, H.J., Han, D., Yang, W.Y., Wu, Y., Yang, S.M., 2013. In vivo delivery of Atoh1 gene to rat cochlea using a dendrimer-based nanocarrier. J. Biomed. Nanotechnol. 9, 1736–1745. https://doi.org/10.1166/jbn.2013.1684

Xie, J., Talaska, A.E., Schacht, J., 2011. New developments in aminoglycoside therapy and ototoxicity. Hear. Res. 281, 28–37. https://doi.org/10.1016/j.heares.2011.05.008

Yang, K.-J., Son, J., Jung, S.Y., Yi, G., Yoo, J., Kim, D.-K., Koo, H., 2018. Optimized phospholipid-based nanoparticles for inner ear drug delivery and therapy. Biomaterials 171, 133–143. https://doi.org/10.1016/j.biomaterials.2018.04.038

Yoon, J.Y., Yang, K.J., Kim, D.E., Lee, K.Y., Park, S.N., Kim, D.K., Kim, J.D., 2015. Intratympanic delivery of oligoarginine-conjugated nanoparticles as a gene (or drug) carrier to the inner ear. Biomaterials 73, 243–253. https://doi.org/10.1016/j.biomaterials.2015.09.025

Yu, Z., Yu, M., Zhang, Z., Hong, G., Xiong, Q., 2014. Bovine serum albumin nanoparticles as controlled release carrier for local drug delivery to the inner ear. Nanoscale Res. Lett. 9, 343. https://doi.org/10.1186/1556-276X-9-343

Zhang, J., Chen, S., Hou, Z., Cai, J., Dong, M., Shi, X., 2015. Lipopolysaccharide-induced middle ear inflammation disrupts the cochlear intra-strial fluid-blood barrier through down-regulation of tight junction proteins. PLoS One 10, e0122572. https://doi.org/10.1371/journal.pone.0122572

Zhang, L., Xu, Y., Cao, W., Xie, S., Wen, L., Chen, G., 2018. Understanding the translocation mechanism of PLGA nanoparticles across round window membrane into the inner ear: A guideline for inner ear drug delivery based on nanomedicine. Int. J. Nanomedicine 13, 479–492. https://doi.org/10.2147/IJN.S154968

Zhang, W., Pyykko, I., Zou, J., Zhang, Y., Loebler, M., Schmitz, K.-P., 2011. Nuclear entry of hyperbranched polylysine nanoparticles into cochlear cells. Int. J. Nanomedicine 6, 535–546. https://doi.org/10.2147/ijn.s16973

Zhang, X., Chen, G., Wen, L., Yang, F., Shao, A., Li, X., Long, W., Mu, L., 2013. Novel multiple agents loaded PLGA nanoparticles for brain delivery via inner ear administration: In vitro and in vivo evaluation. Eur. J. Pharm. Sci. 48, 595–603. https://doi.org/10.1016/J.EJPS.2013.01.007

Zhang, Y., Zhang, W., Johnston, A.H., Newman, T.A., Pyykkö, I., Zou, J., 2012. Targeted delivery of Tet1 peptide functionalized polymersomes to the rat cochlear nerve. Int. J. Nanomedicine 7, 1015–1022. https://doi.org/10.2147/IJN.S28185

Zhang, Y., Zhang, W., Johnston, A.H., Newman, T.A., Pyykkö, I., Zou, J., 2011a. Comparison of the distribution pattern of PEG-b-PCL polymersomes delivered into the rat inner ear via different methods. Acta Otolaryngol. 131, 1249–1256. https://doi.org/10.3109/00016489.2011.615066

Zhang, Y., Zhang, W., Johnston, A.H., Newman, T.A., Pyykkö, I., Zou, J., 2010. Improving the visualization of fluorescently tagged nanoparticles and fluorophore-labeled molecular probes by treatment with CuSO4 to quench autofluorescence in the rat inner ear. Hear. Res. 269, 1–11. https://doi.org/10.1016/j.heares.2010.07.006

Zhang, Y., Zhang, W., Löbler, M., Schmitz, K.-P., Saulnier, P., Perrier, T., Pyykkö, I., Zou, J., 2011b. Inner ear biocompatibility of lipid nanocapsules after round window membrane application. Int.

J. Pharm. 404, 211–219. https://doi.org/10.1016/j.ijpharm.2010.11.006

Zhong, C., Fu, Y., Pan, W., Yu, J., Wang, J., 2019. Atoh1 and other related key regulators in the development of auditory sensory epithelium in the mammalian inner ear: function and interplay. Dev. Biol. 446, 133–141. https://doi.org/10.1016/j.ydbio.2018.12.025

Zou, J., Feng, H., Mannerström, M., Heinonen, T., Pyykkö, I., 2014a. Toxicity of silver nanoparticle in rat ear and BALB/c 3T3 cell line. J. Nanobiotechnology 12, 52. https://doi.org/10.1186/s12951-014-0052-6

Zou, J., Feng, H., Sood, R., Kinnunen, P.K.J., Pyykko, I., 2017a. Biocompatibility of Liposome Nanocarriers in the Rat Inner Ear After Intratympanic Administration. Nanoscale Res. Lett. 12, 372. https://doi.org/10.1186/s11671-017-2142-5

Zou, J., Hannula, M., Misra, S., Feng, H., Labrador, R., Aula, A.S., Hyttinen, J., Pyykkö, I., 2015. Micro CT visualization of silver nanoparticles in the middle and inner ear of rat and transportation pathway after transtympanic injection. J. Nanobiotechnology 13, 5. https://doi.org/10.1186/s12951-015-0065-9

Zou, J., Ostrovsky, S., Israel, L.L., Feng, H., Kettunen, M.I., Lellouche, J.P.M., Pyykkö, I., 2017b. Efficient penetration of ceric ammonium nitrate oxidant-stabilized gamma-maghemite nanoparticles through the oval and round windows into the rat inner ear as demonstrated by MRI. J. Biomed. Mater. Res. Part B Appl. Biomater. 105, 1883–1891. https://doi.org/10.1002/jbm.b.33719

Zou, J., Poe, D., Ramadan, U.A., Pyykkö, I., 2012a. Oval window transport of Gd-DOTA from rat middle ear to vestibulum and scala vestibuli visualized by in vivo magnetic resonance imaging. Ann. Otol. Rhinol. Laryngol. 121, 119–128. https://doi.org/10.1177/000348941212100209

Zou, J., Pyykkö, I., Hyttinen, J., 2016. Inner ear barriers to nanomedicine-augmented drug delivery and imaging. J. Otol. https://doi.org/10.1016/j.joto.2016.11.002

Zou, J., Saulnier, P., Perrier, T., Zhang, Y., Manninen, T., Toppila, E., Pyykkö, I., 2008. Distribution of lipid nanocapsules in different cochlear cell populations after round window membrane permeation. J. Biomed. Mater. Res. Part B Appl. Biomater. 87, 10–18. https://doi.org/10.1002/jbm.b.31058

Zou, J., Sood, R., Ranjan, S., Poe, D., Ramadan, U.A., Kinnunen, P.K.J., Pyykkö, I., 2010a. Manufacturing and in vivo inner ear visualization of MRI traceable liposome nanoparticles encapsulating gadolinium. J. Nanobiotechnology 8, 32. https://doi.org/10.1186/1477-3155-8-32

Zou, J., Sood, R., Ranjan, S., Poe, D., Ramadan, U.A., Pyykkö, I., Kinnunen, P.K.J., 2012b. Size-dependent passage of liposome nanocarriers with preserved posttransport integrity across the middle-inner ear barriers in rats. Otol. Neurotol. 33, 666–673. https://doi.org/10.1097/MAO.0b013e318254590e

Zou, J., Sood, R., Zhang, Y., Kinnunen, P.K.J., Pyykkö, I., 2014b. Pathway and morphological transformation of liposome nanocarriers after release from a novel sustained inner-ear delivery system. Nanomedicine (Lond.) 9, 2143–2155. https://doi.org/10.2217/nnm.13.181

Zou, J., Zhang, W., Poe, D., Qin, J., Fornara, A., Zhang, Y., Ramadan, U.A., Muhammed, M., Pyykkö, I., 2010b. MRI manifestation of novel superparamagnetic iron oxide nanoparticles in the rat inner ear. Nanomedicine 5, 739–754. https://doi.org/10.2217/nnm.10.45

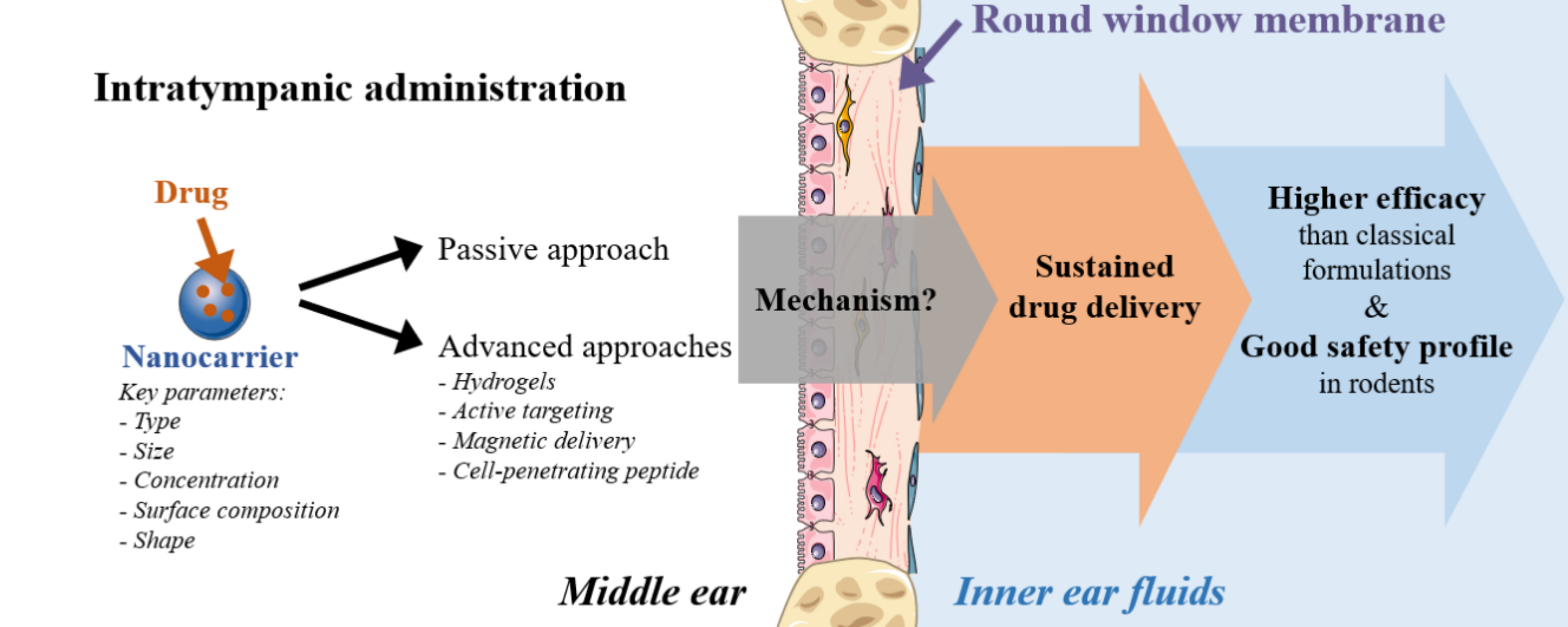
Intratympanic administration
Drug
Nanocarrier
Key parameters:
- Type
- Size
- Concentration
- Surface composition
- Shape
Passive approach
Advanced approaches
- Hydrogels
- Active targeting
- Magnetic delivery
- Cell-penetrating peptide
Round window membrane
Mechanism?
Sustained drug delivery
Higher efficacy
than classical formulations
&
Good safety profile
in rodents
Middle ear
Inner ear fluids